

# Rare-Earth Complexes with Multidentate Tethered Phenoxy-Amidinate Ligands: Synthesis, Structure, and Activity in Ring-Opening Polymerization of Lactide

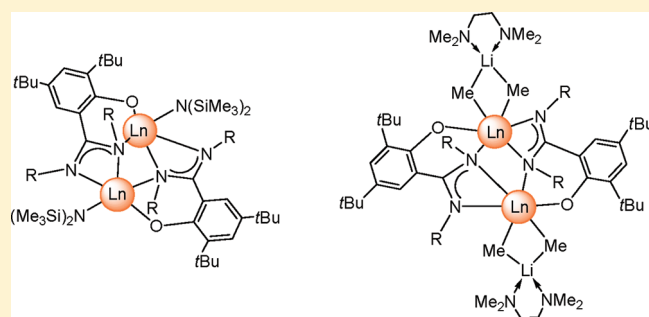
Mikhail Sinenkov,<sup>†</sup> Evgeny Kirillov,<sup>\*,†</sup> Thierry Roisnel,<sup>‡</sup> Georgy Fukin,<sup>†</sup> Alexander Trifonov,<sup>\*,†</sup> and Jean-François Carpentier<sup>\*,†</sup>

<sup>†</sup>G.A. Razuvaev Institute of Organometallic Chemistry of Russian Academy of Sciences, Tropinina 49, GSP-445, 603950 Nizhny Novgorod, Russia

<sup>‡</sup>Catalyse et Organométalliques, CNRS - Université de Rennes 1 - Laboratoire Sciences Chimiques de Rennes (UMR 6226), Campus de Beaulieu, 35042 Rennes Cedex, France

## Supporting Information

**ABSTRACT:** New multidentate tethered amidine-phenol proligands  $\{4,6\text{-}t\text{Bu}_2\text{C}_6\text{H}_2\text{O}-(2\text{-C}(\text{N-R})=\text{N-R})\text{H}_2\}$  ( $\{\text{LON}^{\text{R}}\}\text{H}_2$ ,  $\text{R} = i\text{Pr}$ , cyclohexyl (Cy), 2,6- $i\text{Pr}_2\text{C}_6\text{H}_3$  (Ar)) were synthesized from the corresponding carbodiimines and 2-bromo-2,4-(*tert*-butyl)phenol. Pro-ligands  $\{\text{LON}^{i\text{Pr}}\}\text{H}_2$  and  $\{\text{LON}^{\text{Ar}}\}\text{H}_2$  were metalated by 2 equiv of  $n\text{BuLi}$  to provide the corresponding dilithium salts  $\{\text{LON}^{i\text{Pr}}\}\text{Li}_2$  (**1**) and  $\{\text{LON}^{\text{Ar}}\}\text{Li}_2$  (**2**), which were authenticated by elemental analysis, X-ray crystallography, and NMR spectroscopy. Three different approaches were explored to coordinate these (pro)ligands onto rare earths: salt metathesis, and amine and methane elimination reactions. The salt metathesis reaction between **1** and  $\text{YCl}_3$  afforded the chloro



complex  $[\{\text{LON}^{i\text{Pr}}\}\text{YCl}]_n$  (**3**), which was, in turn, converted into the corresponding amide  $\{\text{LON}^{i\text{Pr}}\}\text{YN}(\text{SiMe}_3)_2$  (**6**) by reaction with  $\text{MN}(\text{SiMe}_3)_2$  ( $\text{M} = \text{Li}, \text{Na}$ ). Similar reactions between **2** and  $\text{YCl}_3$ , followed by recrystallization from DME, led systematically to the isolation of the monoprotonated product, that is, phenoxy-amidino complex  $\{\text{LO}^{\text{H}}\text{N}^{\text{Ar}}\}\text{YCl}_2(\text{DME})$  (**5**). Amine elimination reactions between  $\{\text{LON}^{i\text{Pr}}\}\text{H}_2$  or  $\{\text{LON}^{\text{Cy}}\}\text{H}_2$  and  $\text{Ln}[\text{N}(\text{SiMe}_3)_2]_3$  afforded the corresponding phenoxy-amidinate amides  $\{\text{LON}^{\text{R}}\}\text{LnN}(\text{SiMe}_3)_2$  ( $\text{Ln} = \text{Y}$ ,  $\text{R} = i\text{Pr}$ , **6**;  $\text{R} = \text{Cy}$ , **8**;  $\text{Ln} = \text{Nd}$ ,  $\text{R} = \text{Cy}$ , **9**), whereas the same reaction between  $\{\text{LON}^{\text{Ar}}\}\text{H}_2$  and  $\text{Y}[\text{N}(\text{SiMe}_3)_2]_3$ , under various conditions, always yielded the homoleptic tris(phenoxy-amidinate) complex  $\{\text{LO}^{\text{H}}\text{N}^{\text{Ar}}\}_3\text{Y}$  (**11**). Bimetallic “ate”-complexes  $\{\text{LON}^{\text{R}}\}_2\text{Ln}_2\text{Me}_4\text{Li}_2(\text{TMEDA})_2$  of yttrium (**12** and **13**), neodymium (**14**), samarium (**15**), and  $\{\text{LON}^{i\text{Pr}}\}_2\text{Yb}_2\text{Me}_2(\text{OH})_2\text{Li}_2(\text{TMEDA})_2$  (**16**) were prepared by alkane elimination of the corresponding pro-ligand and  $[\text{Li}(\text{TMEDA})][\text{LnMe}_4]$  complex. Both amido and methyl “ate”-complexes were shown by X-ray diffraction studies to be dimeric in the solid state. The multidentate nature of the ligands in these dimeric species generates a *cis/trans* isomerism related to the nitrogen atoms in the nonsymmetrically coordinated amidinate fragments. Amido complexes **6**, **8**, and **9** are effective initiators for the ring-opening polymerization (ROP) of *racemic* lactide (*rac*-LA), giving atactic or heterotactic-enriched ( $P_t$  up to 76%) polymers with high molecular weights ( $M_n$  up to  $158\,800\text{ g}\cdot\text{mol}^{-1}$ ), but broad molecular weight distributions ( $M_w/M_n = 1.5\text{--}2.8$ ). An effective immortal ROP of *rac*-LA was feasible by combining complex **6** with 5–50 equiv of isopropanol or benzyl alcohol, affording PLAs with well-controlled molecular weights and narrow polydispersities ( $M_w/M_n = 1.11\text{--}1.38$ ).

## INTRODUCTION

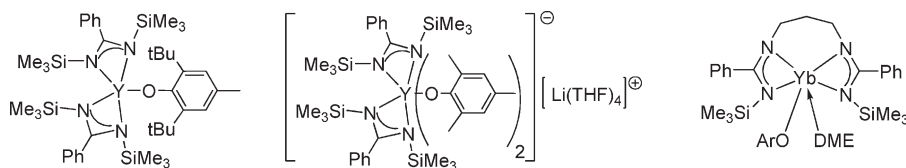
Phenoxide<sup>1</sup> and amidinate<sup>2</sup> anionic ligands are among the most ubiquitous building motifs encountered in the elaboration of rare-earth-based initiators/catalysts that are used in the ring-opening polymerization (ROP) of lactides and other cyclic esters.<sup>3–5</sup> The main advantages of these ancillaries include a highly electron-donating character that results in remarkable stability/robustness of the corresponding metal complexes, and readily tunable steric and electronic features for stabilizing various geometries and oxidation states. On the other hand, there are only few examples of rare-earth complexes that combine

phenoxide and amidinate fragments<sup>5b,d,6</sup> and that proved to be efficient initiators in ROP processes (Scheme 1);<sup>5b,6a,b</sup> in fact, in these cases, the phenoxide group has been proposed to be the true initiating group of the ROP, or the actual nature of the latter initiating group remains still obscure.

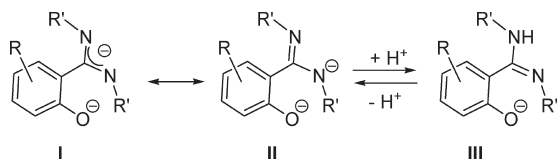
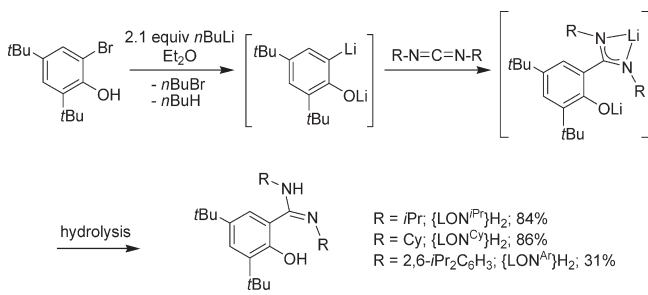
As exemplified exhaustively with the ubiquitous “constrained geometry” Cp-amido dianionic ligands,<sup>7</sup> the implementation of new ligand assemblies incorporating tethered anionic moieties

Received: August 22, 2011

Published: September 22, 2011

Scheme 1. Examples of Rare-Earth Complexes Supported by Phenoxide and Amidinate Ligands<sup>5b,d,6</sup>

## Scheme 2. Some of the Possible Coordination Modes of the Dianionic Phenoxy-Amidinate Ligand (I and II) and a Protonated Monoanionic Form (III)

Scheme 3. Synthesis of Amidine-Phenol Pro-ligands {LON<sup>R</sup>}H<sub>2</sub>

can be of both fundamental and practical value. Herein, we report a new multidentate tethered phenoxy-amidinate dianionic system **I** (Scheme 2). The coordination chemistry of this ligand system with rare-earth metals has been investigated. Two alternative coordination modes of this dianionic ligand (**I** and **II**) and a protonated monoanionic form (**III**, Scheme 2) have been evidenced in complexes of group 3 metals. Preliminary studies on the catalytic activity of some complexes supported by this new tethered phenoxy-amidinate ancillary in the ROP of lactide are reported as well.

## RESULTS AND DISCUSSION

**Synthesis of Pro-ligands.** The amidine-phenol pro-ligands were prepared via a three-step procedure, starting from 2-bromo-4,6-(di-*tert*-butyl)phenol and a set of carbodiimides bearing substituents imparting variable bulkiness and solubility (Scheme 3). The products were isolated in good yields and characterized by NMR spectroscopy and elemental analysis.

**Salt Metathesis Reactions.** Double deprotonation of the amidine-phenol pro-ligands {LON<sup>iPr</sup>}H<sub>2</sub> and {LON<sup>Ar</sup>}H<sub>2</sub> with *n*BuLi, conducted in either toluene or diethyl ether, resulted in the formation of the corresponding dianionic dilithium salts, {LON<sup>iPr</sup>}Li<sub>2</sub> (**1**) and {LON<sup>Ar</sup>}Li<sub>2</sub> (**2**), respectively (Scheme 4).

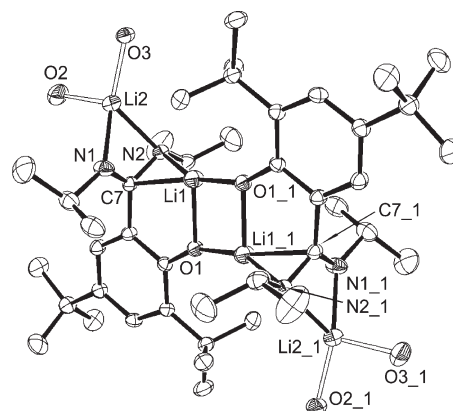


**Figure 1.** Crystal structure of  $[\{LON^{iPr}\}Li_2(THF)_2]_2 \cdot (THF)$  (1) (ellipsoids are drawn at the 50% probability level; all hydrogen atoms, carbon atoms of the coordinated THF molecules, and one THF molecule present in the cell are omitted for clarity).

Both compounds were isolated as white solids and authenticated on the basis of <sup>1</sup>H and <sup>13</sup>C NMR spectroscopies, elemental analysis, and X-ray diffraction studies performed on single crystals of THF adducts  $[\{LON^{iPr}\}Li_2(THF)_2]_2 \cdot (THF)$  and  $\{LON^{Ar}\}Li_2(THF)_3$ , obtained by recrystallization of **1** and **2**, respectively, from THF/hexanes (1:1) mixtures.

The solid-state structure of  $[\{LON^{iPr}\}Li_2(THF)_2]_2 \cdot (THF)$  is dimeric, featuring a crystallographic inversion center that lies at the center of the Li(1)–O(1)–Li(1\_1)–O(1\_1) plane (Figure 1; for crystallographic details, see Tables S1 and S2, Supporting Information). Two of the four Li atoms in the dimeric structure are bound to the oxygen atoms of the bridging phenoxides (Li–O = 1.832(3) and 1.979(3) Å<sup>8</sup>) and to one carbon and one nitrogen atom (Li–C(7) = 2.236(3), Li–N(2) = 2.172(3) Å, respectively) of the anionic amidinate group. Two other Li atoms are also four-coordinated and bound each to the nitrogen atoms of the amidinate groups (Li–N = 2.019(3) and 2.042(3) Å<sup>9</sup>) and oxygen atoms of THF molecules (Li–O = 1.944(3) and 2.009(3) Å).

The <sup>1</sup>H NMR spectrum of {LON<sup>iPr</sup>}Li<sub>2</sub> (**1**) in THF-*d*<sub>6</sub> displayed broadened resonances in the 298–353 K temperature range. This feature is indicative of a fluxional dynamic phenomenon that can be attributed to a haptotropic rearrangement process involving the amidinate moieties, and which is relatively slow on the NMR time scale.

On the other hand, the dilithium salt {LON<sup>Ar</sup>}Li<sub>2</sub>(THF)<sub>3</sub> (**2**) is monomeric in the solid state (Figure 2). The amidinate moiety in **2**, despite its anionic character, is nonsymmetrically coordinated with metal atoms. The differences in the C–N bond lengths (N(1)–C(7) = 1.368(4) Å, N(2)–C(7) = 1.314(4) Å) argue that most of the negative charge of the amidinate moiety is located mainly on the nitrogen atom N(1), onto which are actually

## Scheme 4. Synthesis of the Dilithium Salts 1 and 2 and Yttrium Complexes 3–5 Derived Thereof

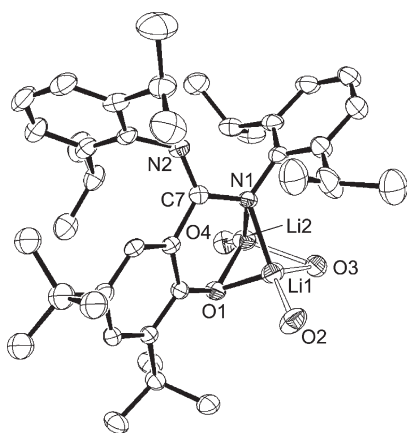
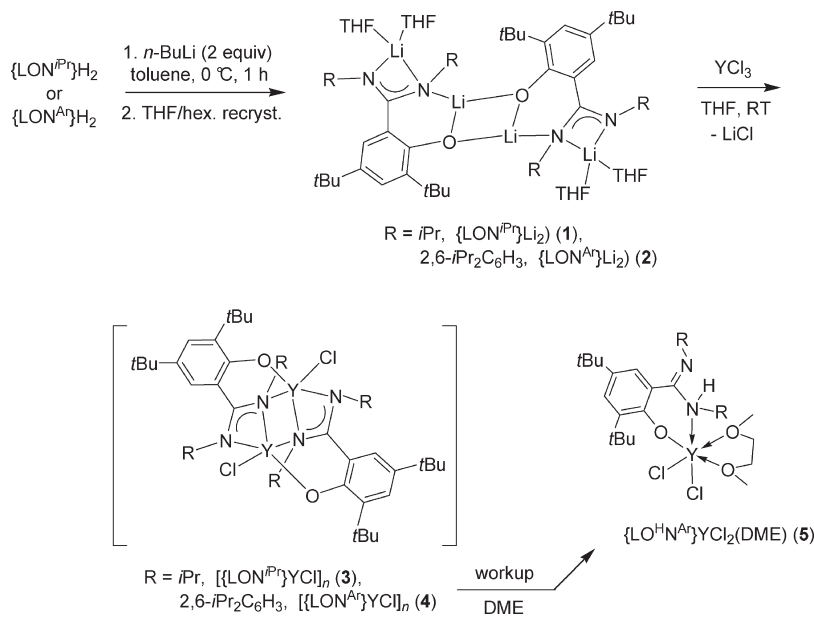


**Figure 2.** Crystal structure of  $\{LON^{Ar}\}Li_2(THF)_3$  (2) (ellipsoids are drawn at the 50% probability level; all hydrogen atoms and carbon atoms of the coordinated THF molecules, as well as those of the disordered *t*Bu and *i*Pr groups, are omitted for clarity).

bound the two Li atoms. Both Li atoms are four-coordinated and bound to the same oxygen and nitrogen atoms of the dianionic ligand, however, in a rather dissymmetric manner. For instance, the Li(1)–O(1) distance (1.926(6) Å) is longer than the Li(2)–O(1) one (1.818(6) Å),<sup>8</sup> whereas the Li(1)–N(1) distance (2.018(6) Å) is shorter as compared with the Li(2)–N(1) one (2.182(6) Å).<sup>9</sup> Also, a dynamic behavior similar to the one observed for **1** was evidenced for **2** by <sup>1</sup>H NMR spectroscopy in THF-*d*<sub>8</sub> in the temperature range of 298–353 K.

The reaction of dilithium salt **1** with  $YCl_3$  in THF gave the corresponding chloro complex  $\{[LON^{Pr^i}YCl]_n\}$  (**3**) in 56% isolated yield (Scheme 4). This compound was characterized by <sup>1</sup>H and <sup>13</sup>C NMR spectroscopies and elemental analysis. All the efforts to obtain crystals of **3** suitable for X-ray diffraction study failed. A similar reaction between **2** and  $YCl_3$  resulted, after workup and a subsequent recrystallization of the product from

DME, in isolation of the unexpected complex  $\{LO^H N^{Ar}\}YCl_2(DME)$  (**5**) in 32% yield (Scheme 4). Repeated experiments, with special care to avoid adventitious hydrolysis, resulted in a similar outcome. Apparently, the high instability of the dilithium salt **2** and/or its yttrium complex **4** accounts for the observed protonolysis reaction, although the exact stage and nature of the proton source in this latter reaction could not be unambiguously identified.

The solid-state structure of **5** has been determined (Figure 3; see Tables 1 and 2 for main bond distances and angles) and revealed the yttrium atom in a distorted octahedral coordination environment, with the ligand nitrogen and DME oxygen atoms occupying the axial positions, while two oxygen atoms of the ligand and DME as well as two terminal chloro ligands lie in the equatorial positions. The Y(1)–O(1) bond length in **5** (2.129(2) Å) is similar to the values of covalent bonds reported for related six- and seven-coordinated yttrium complexes with phenoxide and salicylaldehyde ligands (2.114–2.166 Å).<sup>10</sup> The Y(1)–N(1) bond (2.300(3) Å) is much shorter than the Y–N coordination bonds (2.515–2.661 Å) in the latter compounds<sup>10</sup> and is comparable to the Y–N distances reported for yttrium amidinate and guanidinate complexes (2.284–2.469 Å).<sup>11</sup> The Y–Cl bond lengths in **5** (2.584(1) and 2.614(1) Å) fall into the regular range for terminal Y–Cl bonds in six-coordinated complexes.<sup>12</sup> Simple electroneutrality considerations imply the existence of a protonated amidinate fragment (i.e., R–N=C(R′)–NHR) in **5**, although the X-ray diffraction study did not allow us to localize this amino hydrogen, most likely due to its proximity to the heavy metal atom. However, the geometric features of the NCN fragment differ considerably from that described for *anionic* amidinate moieties with similar monodentate coordination<sup>13</sup> and are indicative of its protonated form at N(2). In fact, the N–C bonds within the NCN fragment are quite inequivalent (N(1)–C(7) = 1.389(4) Å vs N(2)–C(7) = 1.306(4) Å) and differ noticeably from the corresponding distances in the related free amidine (1.321(3) and 1.352(3) Å).<sup>14</sup>

To access complexes potentially useful for ROP catalysis, the chloro complex **3** was treated with  $MN(\text{SiMe}_3)_2$  (where  $M = \text{Li}, \text{Na}$ ); the corresponding amido complex  $\{\text{LON}^{\text{ipr}}\}\text{YN}(\text{SiMe}_3)_2$  (**6**) was thus recovered in 78% yield (Scheme 5). Despite its very high solubility in aliphatic hydrocarbons (pentane, hexanes), single crystals of **6** suitable for X-ray diffraction studies were successfully grown. The complex is dimeric in the solid state, and its structure is depicted in Figure 4. The molecule of **6** features a crystallographic  $C_2$ -symmetry axis that passes through the center of the  $\text{Y}(1)-\text{N}(2_1)-\text{Y}(1_1)-\text{N}(2)$  core (this makes the molecule chiral, and the unit cell of **6** contains the two enantiomeric molecules). Each one of the two yttrium atoms is in a

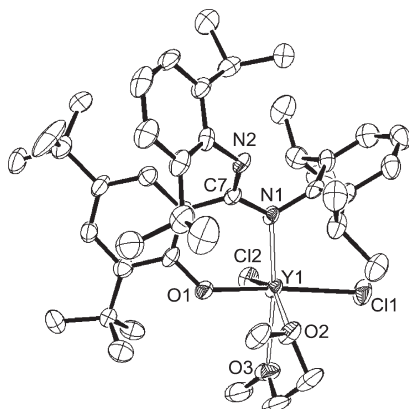


**Figure 3.** Crystal structure of  $\{\text{LO}^{\text{H}}\text{N}^{\text{Ar}}\}\text{YCl}_2(\text{DME})$  (**5**) (ellipsoids are drawn at the 50% probability level; H atoms are omitted for clarity).

distorted trigonal bipyramidal environment, with one oxygen and two nitrogen atoms of the phenoxide and chelating amidinate moieties, respectively, lying in the equatorial plane, and two axial nitrogen atoms of the  $(\text{Me}_3\text{Si})_2\text{N}$  and amidinate groups. Unlike in mono- and bisamidinate yttrium complexes,<sup>6a</sup> the coordination of the amidinate moiety to the metal center in **6** is non-symmetric, as indicated by inequivalent  $\text{Y}-\text{N}(\text{amidinate})$  bonds (2.363(4), 2.437(4), 2.371(3), and 2.459(4) Å) and  $\text{C}-\text{N}$  bonds ( $\text{C}(7_1)-\text{N}(1_1) = 1.304(5)$  Å,  $\text{C}(7_1)-\text{N}(2_1) = 1.384(6)$  Å,  $\text{C}(7)-\text{N}(1) = 1.287(5)$  Å,  $\text{C}(7)-\text{N}(2) = 1.394(6)$  Å) in the amidinate fragment. The  $\text{Y}-\text{N}(\text{amido})$  bond length (2.228(4), 2.238(4) Å) is in agreement with the values reported for yttrium amido complexes.<sup>15</sup>

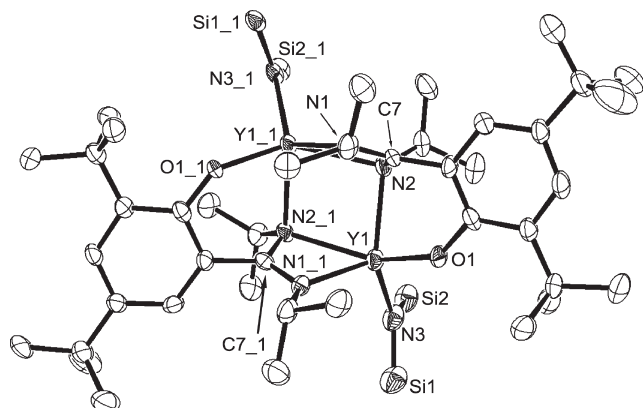
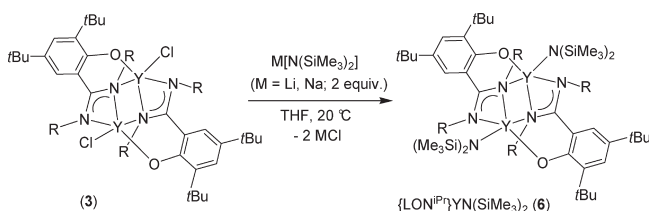
The  $^1\text{H}$  and  $^{13}\text{C}$  NMR spectra of **6**, in  $\text{C}_6\text{D}_6$  or in  $\text{THF}-d_8$  at room temperature, were consistent with an average  $C_2$ -symmetric structure in solution on the NMR time scale (Figures S10–S12, respectively; see the Supporting Information). Key  $^1\text{H}$  NMR

**Table 2.** Selected Bond Distances (Å) and Angles (°) for Complexes **5**, **7**, and **10**

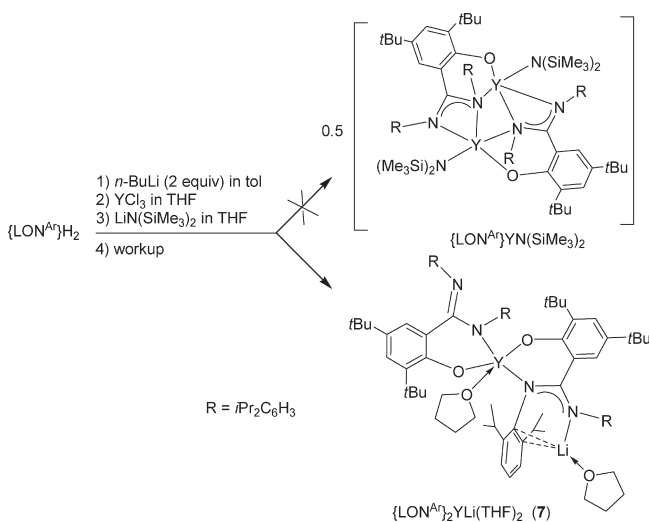
	<b>5</b>	<b>7</b>	<b>10</b>
$\text{M1}-\text{Cl2}$	2.5842(11)		
$\text{N1}-\text{C7}$	1.389(4)	1.393(3)	1.337(4)
$\text{N2}-\text{C7}$	1.306(4)	1.297(3)	1.352(4)
$\text{M1}-\text{O2}$		2.1488(18)	
$\text{M1}-\text{N3}$		2.411(2)	
$\text{Li1}-\text{N4}$		1.983(6)	
$\text{Li1}-\text{N2}$			2.118(5)

**Table 1.** Selected Bond Distances (Å) and Angles (°) for Dimeric Complexes **6**, **9**, **12**, **13**, and **16**

	<b>6</b>	<b>9</b>	<b>12</b>	<b>13</b>	<b>16</b>
$\text{M}(1)-\text{O}(1)$	2.124(3)	2.196(3)	2.1723(11)	2.159(2)	2.1123(14)
$\text{M}(1)-\text{N}(1_1)$	2.363(4)	2.445(4)	2.4967(13)	2.398(3)	2.3720(17)
$\text{M}(1)-\text{N}(2_1)$	2.437(4)	2.571(4)	2.4575(13)	2.474(3)	2.4183(16)
$\text{M}(1)-\text{N}(2)$	2.473(4)	2.528(4)	2.5525(13)	2.518(3)	2.4648(16)
$\text{M1}_1-\text{O1}_1$	2.113(3)	2.216(3)	2.1723(11)	2.168(2)	2.1173(15)
$\text{M}(1_1)-\text{N}(1)$	2.372(3)	2.471(4)	2.4967(13)	2.423(3)	2.3671(16)
$\text{M}(1_1)-\text{N}(2)$	2.459(4)	2.551(4)	2.4575(13)	2.453(3)	2.4228(16)
$\text{M}(1_1)-\text{N}(2_1)$	2.447(4)	2.589(4)	2.5525(13)	2.525(3)	2.4694(17)
$\text{M}(1)-\text{C}(22)$			2.4943(18)	2.532(4)	2.474(2)
$\text{M}(1)-\text{C}(23)$			2.4746(18)	2.491(4)	
$\text{M}(1)-\text{N}(3)$	2.228(4)	2.344(4)			
$\text{M}(1_1)-\text{N}(3_1)$	2.238(4)	2.316(4)			
$\text{M}(1)-\text{O}(2)$					2.5481(16)
$\text{N}(1)-\text{C}(7)$	1.286(6)	1.311(6)	1.313(2)	1.315(5)	1.312(3)
$\text{N}(2)-\text{C}(7)$	1.394(6)	1.404(5)	1.375(2)	1.392(5)	1.393(3)
$\text{N}(1_1)-\text{C}(7_1)$	1.304(5)	1.314(6)	1.313(2)	1.299(4)	1.306(3)
$\text{N}(2_1)-\text{C}(7_1)$	1.384(6)	1.381(6)	1.375(2)	1.382(5)	1.393(3)
$\text{N}(1_1)-\text{M}(1)-\text{N}(2_1)$	56.48(13)	53.66(12)	54.22(4)	55.18(10)	56.36(5)
$\text{N}(1_1)-\text{C}(7_1)-\text{N}(2_1)$	115.3(4)	114.5(4)	114.28(14)	114.7(3)	113.82(18)
$\text{C}(7_1)-\text{M}(1)-\text{O}(1)$	122.86(13)	121.26(12)	159.84(4)	118.62(10)	120.92(6)
$\text{C}(7_1)-\text{M}(1)-\text{N}(3)$	111.52(14)	115.42(13)			
$\text{O}(1)-\text{M}(1)-\text{N}(3)$	109.34(13)	112.88(13)			
$\text{C}(22)-\text{M}(1)-\text{C}(23)$			91.70(6)	89.88(13)	
$\text{Li}(1)-\text{C}(22)-\text{M}(1)$			80.25(10)	79.96	80.80(13)
$\text{C}(7_1)-\text{M}(1)-\text{Li}(1)$			105.78(7)	121.28	120.41(9)
$\text{O}(1)-\text{M}(1)-\text{Li}(1)$			92.99(6)	110.49	107.67(8)

**Scheme 5. Synthesis of Amido Yttrium Complex  $\{LON^{iPr}\}_2Yn(SiMe_3)_2$  (6) by Salt Metathesis**


**Figure 4.** Molecular structure of  $\{LON^{iPr}\}_2Yn(SiMe_3)_2$  (6) (ellipsoids are drawn at the 50% probability level; H atoms and Me groups of  $Me_3Si$  units are omitted for clarity).

**Scheme 6. Attempted “One-Pot” Salt Metathesis Reaction Towards Complex  $\{LON^{Ar}\}_2YLi(THF)_2$  and Formation of  $\{LON^{Ar}\}_2YLi(THF)_2$  (7)**


resonances include (a) two singlets for  $H^3$  and  $H^5$  hydrogens of the phenoxide groups, (b) one broadened multiplet for the  $CH(CH_3)$  isopropyl groups, (c) two sharp singlets for the  $tBu$  groups, (d) one doublet for the  $CH(CH_3)$  isopropyl groups, and (e) a unique singlet resonance for the  $SiMe_3$  groups.

Attempts to synthesize an amido complex  $\{LON^{Ar}\}_2Yn(SiMe_3)_2$  supported by a bulkier  $LON^{Ar}$  ligand system were undertaken via

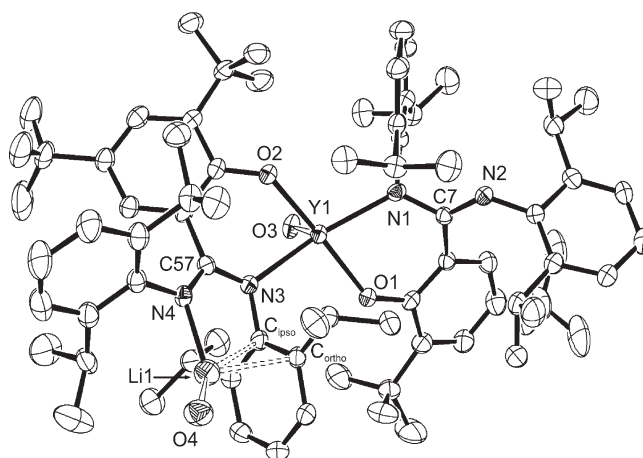
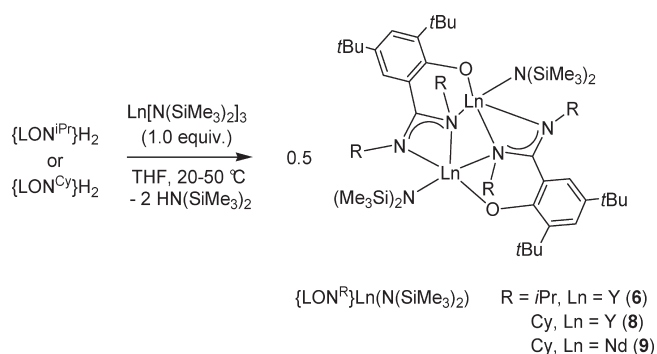


**Figure 5.** Molecular structure of  $\{LON^{Ar}\}_2YLi(THF)_2$  (7) (ellipsoids are drawn at the 50% probability level; all hydrogen atoms and carbon atoms of the coordinated THF molecules, as well as those of the disordered  $tBu$  groups, are omitted for clarity).

a one-pot reaction, to minimize protonolysis problems encountered in the case of 4/5 (vide supra) (Scheme 6). However, this procedure led to the heterobimetallic bis-ligand “ate”-complex  $\{LON^{Ar}\}_2YLi(THF)_2$  (7), isolated in 33% yield, which was authenticated by elemental analysis, NMR spectroscopy, and an X-ray diffraction study.

The solid-state structure of 7 revealed a five-coordinate species, in which the yttrium center lies in a distorted tetragonal pyramidal environment (Figure 5). Two oxygen and two nitrogen atoms of the two chelating ligands occupy the equatorial plane of this pyramid, while the oxygen atom of the coordinated THF molecule is in the axial position ( $Y(1)-O(3) = 2.287(2) \text{ \AA}$ ). Each phenoxy-amidinate ligand in 7 is connected to the yttrium center by one  $Y-O$  and one  $Y-N$  bond, while the second amidinate nitrogen does not bind to yttrium. The two dianionic ligands are not equivalent since the second nitrogen of one of them (N(4)) is also bound with a lithium atom. Despite this fact, both ligands display quite similar  $Y-O$  bond distances ( $2.154(2)$  and  $2.149(2) \text{ \AA}$ ) and their bonding situation is consistent with phenoxy-amido character.<sup>16</sup> However, the geometric parameters of the NCN fragments in the two ligands differ noticeably: in one moiety, the  $C(7)-N(2)$  bond is significantly shorter than the  $C(7)-N(1)$  ( $1.297(3)$  vs  $1.393(3) \text{ \AA}$ ), suggesting a double character for the former bond. On the other hand, in the moiety that binds both yttrium and lithium atoms, the  $Y(1)-N(3)$  bond ( $2.411(2) \text{ \AA}$ ) is almost  $0.1 \text{ \AA}$  longer than the  $Y(1)-N(1)$  one. In the amidinate group of this ligand, the double bond is partially delocalized within the  $N(3)-C(57)-N(3)$  fragment, which is in agreement with the corresponding bond lengths  $C(57)-N(3)$  ( $1.370(3) \text{ \AA}$ ) and  $C(57)-N(4)$  ( $1.329(3) \text{ \AA}$ ). The lithium atom in this molecule is bound with one of the two nitrogen atoms of the amidinate group ( $Li(1)-N(4) = 1.983(6) \text{ \AA}$ ) and also accommodates a THF molecule ( $Li(1)-O(4) = 1.887(6) \text{ \AA}$ ). In addition, the lithium atom exhibits short interactions with the  $\pi$ -system of the adjacent aromatic ring of the di(*iso*-propyl)-anilinic moiety ( $Li(1)-C_{ipso} = 2.382(6) \text{ \AA}$  and  $Li(1)-O_{ortho} = 2.415(6) \text{ \AA}$ ). These distances are in good agreement with  $Li-C(\text{arene})$  distances ( $2.15-2.651 \text{ \AA}$ ) observed in arene-substituted amido and amidinate<sup>17</sup> and in arene<sup>18</sup> complexes of lithium.

**Scheme 7. Synthesis of Amide Complexes**  
 $\{LON^R\}_2LnN(SiMe_3)_2$  by Amine Elimination Reactions



**Amine Elimination Approach.** Alternatively, amine elimination reactions were investigated as an efficient one-step route toward the compounds targeted for ROP catalysis. The NMR-scale reactions between  $Y[N(SiMe_3)_2]_3$  and  $\{LON^{iPr}\}_2H_2$  or  $\{LON^{Cy}\}_2H_2$  pro-ligands in  $C_6D_6$  were sluggish at room temperature and yielded in 24 h mixtures of at least two unidentified products containing unreacted  $-NHR$  amino groups (R = *i*Pr or Cy) of the amidinate moieties. Further heating of these mixtures over prolonged reaction times (ca. 50 h) did not improve either the selectivity or the yield of these reactions. On the other hand, the same reactions, carried out in THF- $d_8$  at room temperature or at 50 °C over 48 h, resulted in the selective formation of the corresponding amido complexes  $\{LON^R\}_2YN(SiMe_3)_2$  (R = *i*Pr, **6**; Cy, **8**) (Scheme 7). Following a similar approach, the neodymium complex  $\{LON^{Cy}\}_2NdN(SiMe_3)_2$  (**9**) was isolated in 61% yield. The solution structure of yttrium complex **8** was established by  $^1H$  and  $^{13}C$  NMR spectroscopies, whereas the NMR data obtained for **9** were not informative due to extremely broad and unresolved resonances that resulted from the strong paramagnetism of neodymium. In  $C_6D_6$  solution, **8** behaves as an average  $C_2$ -symmetric species, similarly to **6** (Figures S15 and S16; see the Supporting Information). A moderate fluxional behavior, assigned to hindered motion of the cyclohexyl groups, was observed for **8** in  $C_6D_6$  solution at room temperature.

The solid-state structure of neodymium compound **9** was established by X-ray diffraction (Figure 6). Two crystallographically independent enantiomeric molecules featuring very similar geometrical parameters were found in the crystal cell, and only one of these is discussed hereafter. The overall geometry of **9** is quite similar to that of **6** in terms of relative atom placements and bonding. That is, the dimeric structure is composed of two metal centers grasped into a core by bridging  $N,N'$ -dihapto-amidinate groups of two phenoxy-amidinate ligands. The values of the Nd–O(1) and Nd–O(1<sub>1</sub>) bond lengths (2.196(3) and 2.216(3) Å, respectively) in **9** are close to those formerly reported for neodymium phenoxides,<sup>2d,19</sup> whereas the Nd–N(amidinate) bond distances (2.445(4), 2.571(4), 2.551(4), and 2.471(4) Å) fall in the range characteristic for those in neodymium amidinates and guanidinates.<sup>7e,20</sup> Expectedly, the bond lengths between the central carbon atom of the amidinate fragment and the  $\mu$ -bridging nitrogen atom (C(7)–N(2) = 1.405(5) Å and C(7<sub>1</sub>)–N(2<sub>1</sub>) = 1.382(6) Å, respectively) are longer than the terminal ones (C(7)–N(1) = 1.311(6) Å and C(7<sub>1</sub>)–N(1<sub>1</sub>) = 1.314(6) Å).

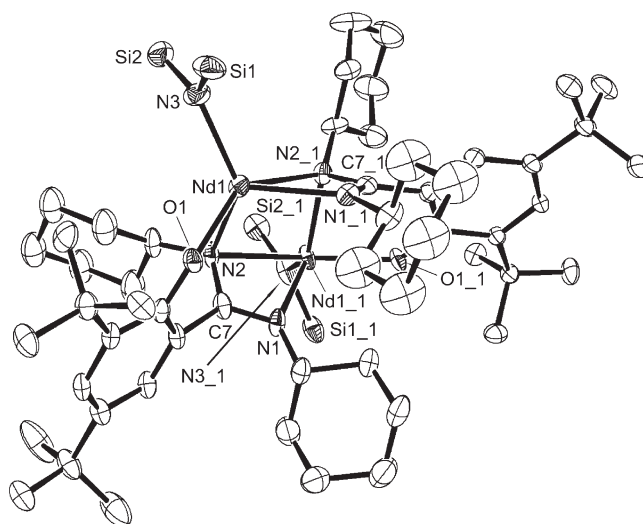
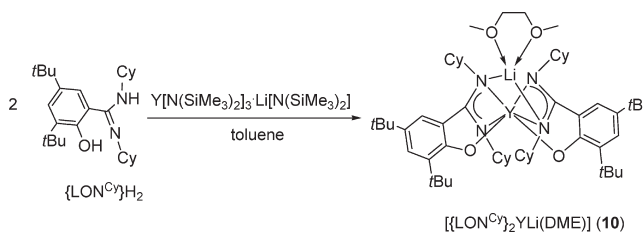


**Figure 6.** Molecular structure of  $\{LON^{Cy}\}_2NdN(SiMe_3)_2$  (**9**) (ellipsoids are drawn at the 50% probability level; H atoms and Me groups of  $Me_3Si$  units are omitted for clarity).

**Scheme 8. Formation of Yttrium “ate”-Complex**  
 $\{LON^{Cy}\}_2YLi(DME)$  (**10**)



In the course of purification of complex **8**, the treatment of its hexane solution with DME resulted in the formation of colorless crystals of heterobimetallic complex  $\{LON^{Cy}\}_2YLi(DME)$  (**10**) (Scheme 8), which was isolated in 5% yield. Complex **10** is hardly soluble in DME and THF and is insoluble in toluene and hexane. Obviously, the presence of residual  $LiN(SiMe_3)_2$  in the starting  $Y[N(SiMe_3)_2]_3$  accounted for the formation of **10**. Complex **10** was prepared purposely in 45% yield via the reaction between  $YCl_3$  and 2 equiv of  $\{LON^{Cy}\}_2Li_2$ .<sup>21</sup>

An X-ray diffraction study of suitable crystals of **10** revealed that this compound is a heterobimetallic complex containing lithium and yttrium atoms connected together by two dianionic phenoxy-amidinate ligands, which are coordinated to the yttrium center in a bidentate  $\kappa^3$ -fashion (Figure 7). The molecule of **10** features  $C_2$  symmetry in the solid state, with the corresponding axis passing through the yttrium and lithium centers and the midpoint of the C–C bond of the coordinated DME molecule. As a result, **10** exists as a racemic mixture of two enantiomers; both of them are found in the unit cell. In the series of phenoxy-amidinate rare-earth complexes reported in this paper, compound **10** is the sole example where all three donor atoms (N,N,O) are bound to the same metal atom. At the same time, one of the nitrogen atoms of each amidinate moiety is coordinated to the lithium ion, thus bridging it with yttrium. The Y(1)–O(1) bond in **10** (2.174(2) Å) is somewhat longer than the corresponding bond in heterobimetallic complex **7**. The four Y–N

bonds are inequivalent, and the distance between the yttrium atom and terminal nitrogen ( $Y(1)-N(21) = 2.362(3) \text{ \AA}$ ) is expectedly shorter as compared with the one  $\mu$ -bridging between the yttrium and lithium atoms ( $Y(1)-N(31) = 2.521(3) \text{ \AA}$ ). The C–N bond lengths within the amidinate fragments are also slightly different ( $C(7)-N(21) = 1.337(4) \text{ \AA}$  vs  $C(7)-N(31\_2) = 1.352(4) \text{ \AA}$ ).

When the bulkier pro-ligand  $\{LON^{Ar}\}_2H_2$  was used in the amine elimination reaction with  $Y[N(SiMe_3)_2]_3$ , the sole product observed was the homoleptic complex  $\{LO^H N^{Ar}\}_3Y$  (**11**) (Scheme 9). Tuning the reaction conditions (more elevated temperatures, extended reaction times, nature of solvents) did not affect the final outcome.<sup>22</sup> The  $^1H$  and  $^{13}C$  NMR data for **11** ( $C_6D_6$ , room temperature) were consistent with an average symmetric species on the NMR time scale in which all the three ligands are monoanionic, chelating the metal center with the imino nitrogen atoms. Diagnostic  $^1H$  NMR resonances include (a) six multiplets for six different types of aromatic hydrogens, (b) one singlet for the amino protons of the pendant  $NH(iPr_2C_6H_3)$  groups, (c) two septets for the methine protons of the *iPr* groups, (d) two singlets for the *t*Bu groups, and (e) four doublets for the methyl hydrogens of the *iPr* groups.

**Alkane Elimination Approach.** Recent studies in the chemistry of groups 3 and 4 metals have shown the alkane elimination approach, using homoleptic  $MR_3$  and  $MR_4$  precursors, respectively, and amidine-based pro-ligands, to be a versatile route toward different classes of amidinate complexes.<sup>23,24</sup> Heteroleptic

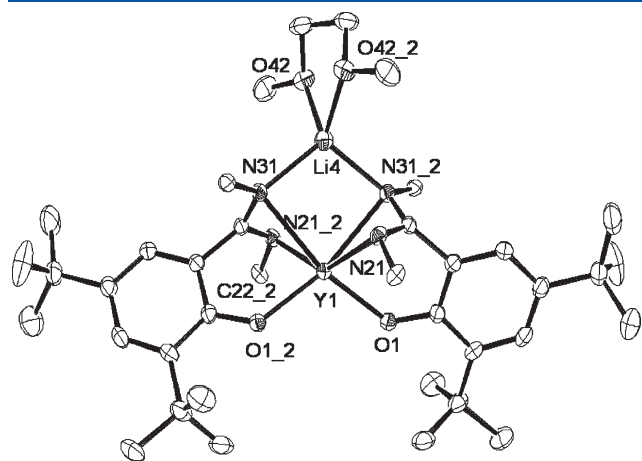
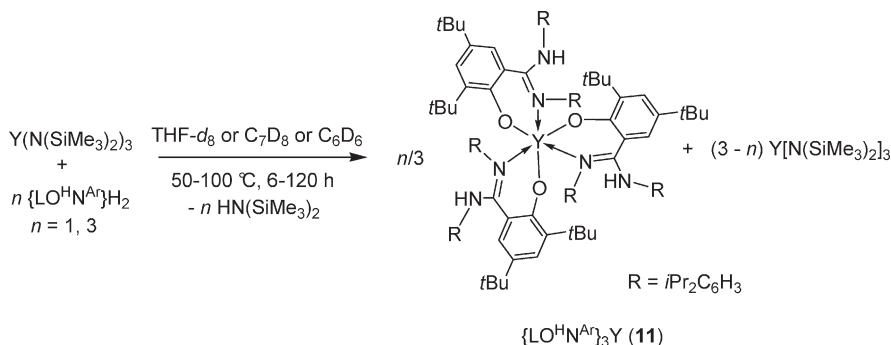


**Figure 7.** Molecular structure of  $\{LON^{Cy}\}_2YLi(DME)$  (**10**) (H atoms and cyclohexyl rings are omitted for clarity; ellipsoids are drawn at the 50% probability level).

**Scheme 9. Amine Elimination Reaction between  $\{LON^{Ar}\}_2H_2$  and  $Y[N(SiMe_3)_2]_3$**

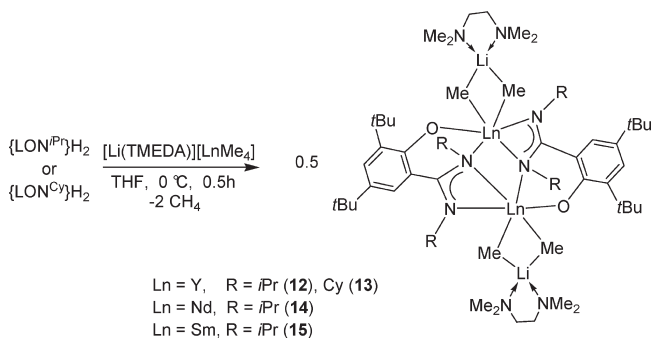


methyl “ate”-complexes  $[Li(TMEDA)][LnR_4]$  ( $R = Me, CH_2SiMe_3$ ) have been scrutinized in our previous studies as convenient starting materials for preparing highly reactive lanthanide complexes being able to promote enantioselective intramolecular olefin hydroamination.<sup>25</sup>

Accordingly, a series of methyl “ate”-complexes  $\{LON^R\}_2Ln_2Me_4Li_2(TMEDA)_2$  of yttrium (**12** and **13**), neodymium (**14**), and samarium (**15**) were prepared in high yields via a one-step methane-elimination reaction between the pro-ligands  $\{LON^{iPr}\}_2H_2$  and  $\{LON^{Cy}\}_2H_2$  with the in situ generated  $[Li(TMEDA)][LnMe_4]$ <sup>25b</sup> (Scheme 10). These compounds are readily soluble in diethyl ether and aromatic hydrocarbons (toluene and benzene). They were characterized by elemental analysis, NMR spectroscopy (for diamagnetic species), and crystal structure determinations for **12** and **13**.

Crystals of **12** and **13** suitable for X-ray diffraction studies were obtained by cooling concentrated solutions of the complexes in diethyl ether at  $-20 \text{ }^\circ\text{C}$ . Both compounds crystallize as solvates containing one molecule of diethyl ether per unit cell. These complexes adopt dimeric structures in the solid state (Figures 8 and 9, respectively). The dimers formed via  $\mu$ -bridging of the dianionic phenoxy-amidinate ligands, with the amidinate and alkoxy units of a given ligand bound to two different yttrium atoms. One of the two nitrogen atoms of each amidinate fragments is  $\mu$ -bridging between the two yttrium atoms, while the second one is terminal. In addition, two  $\mu$ -bridging methyl groups connect the yttrium center with  $Li(TMEDA)$ . Each six-coordinate yttrium atom in  $12 \cdot (Et_2O)$  and  $13 \cdot (Et_2O)$  adopts a trigonal prismatic geometry. The molecule of **12** has a crystallographic inversion center lying at the center of the  $Y(1)-N(2)-Y(1\_1)-N(2\_1)$  plane. On the other hand, the molecule of **13** is  $C_2$ -symmetric with the corresponding axis passing perpendicularly through the

**Scheme 10. Synthesis of Heterometallic Methyl “ate”-Complexes  $\{LON^R\}_2Ln_2Me_4Li_2(TMEDA)_2$  (**12–15**)**



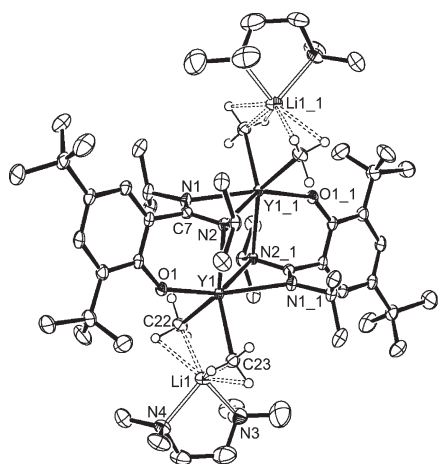


**Figure 8.** Molecular structure of  $\{\text{LON}^{\text{iPr}}\}_2\text{Y}_2\text{Me}_4\text{Li}_2(\text{TMEDA})_2 \cdot (\text{Et}_2\text{O})$  (**12**) (ellipsoids are drawn at the 50% probability level; H atoms, except those of the bridging methyl groups, and a molecule of  $\text{Et}_2\text{O}$  are omitted for clarity).

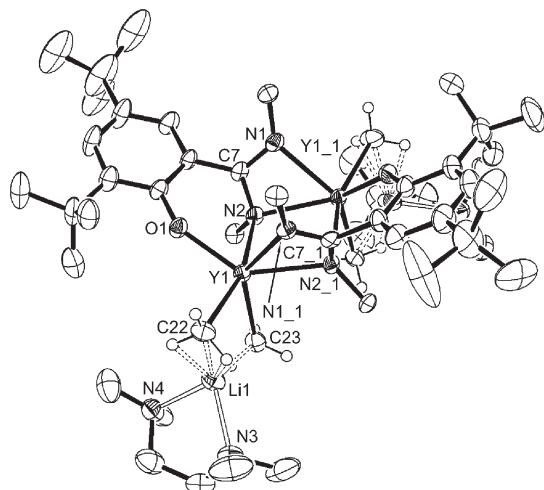


**Figure 9.** Molecular structure of  $\{\text{LON}^{\text{Cy}}\}_2\text{Y}_2\text{Me}_4\text{Li}_2(\text{TMEDA})_2 \cdot (\text{Et}_2\text{O})$  (**13**) (ellipsoids are drawn at the 50% probability level; H atoms, except those of the bridging methyl groups, cyclohexyl groups, and a molecule of  $\text{Et}_2\text{O}$  are omitted for clarity).

center of the  $\text{Y}(1)–\text{N}(2)–\text{Y}(1)–\text{N}(2)$  core. The average  $\text{Y}–\text{C}(\text{methyl})$  bond length in **12** (2.484 Å) is somewhat shorter than that in **13** (2.515 Å),<sup>26</sup> whereas on the contrary, the average  $\text{Y}–\text{N}$  distance is longer in **12** (2.476 Å) than in **13** (2.437 Å). The  $\text{Y}–\text{O}$  bond distances in **12** (2.172(1) Å) and **13** (2.168(2) and 2.159(2) Å) are longer with respect to those in the five-coordinate complex **6** (2.113(3) and 2.124(3) Å) and are also close to those in the six-coordinate **7** (2.154(2) and 2.149(2) Å).

The composition and symmetry of dimeric **12** and **13** found in the solid state are retained in solution, as judged by  $^1\text{H}$  and  $^{13}\text{C}$  NMR spectroscopies. Both the  $^1\text{H}$  and the  $^{13}\text{C}$  NMR spectra of **12** and **13**, recorded in  $\text{C}_6\text{D}_6$  at room temperature, exhibited only one set of resonances for each type of nucleus (Figures S21, S22 and Figures S23, S24, respectively; see the Supporting Information). Also, as a result of fast fluxional dynamics on the NMR time scale, the methyl groups appeared as a single resonance in the  $^1\text{H}$  and  $^{13}\text{C}$  NMR spectra of both **12** and **13**.

### Scheme 11. Synthesis of Heterometallic Methyl-Hydroxo “ate”-Complex $\{\text{LON}^{\text{iPr}}\}_2\text{Yb}_2\text{Me}_2(\text{OH})_2\text{Li}_2(\text{TMEDA})_2$ (**16**)

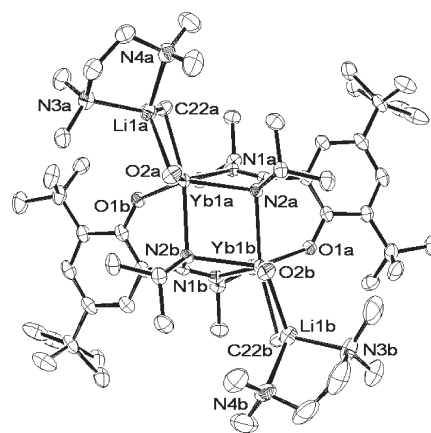
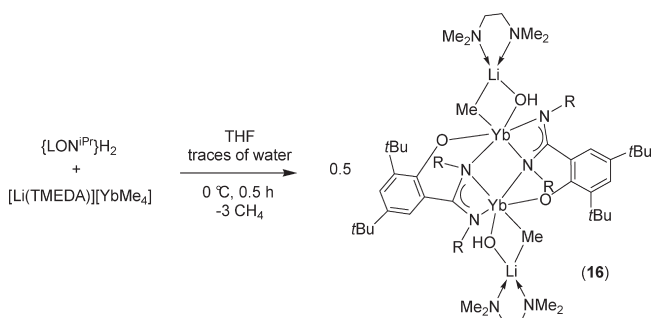
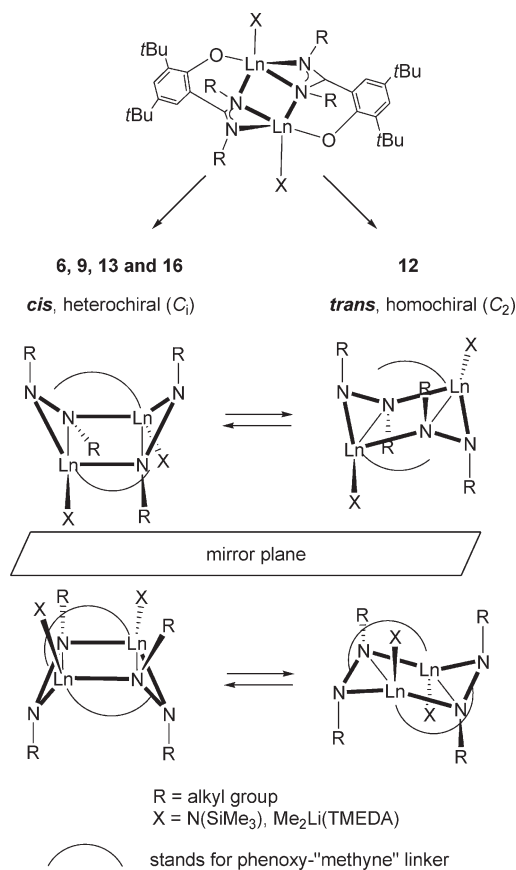


**Figure 10.** Molecular structure of  $\{\text{LON}^{\text{iPr}}\}_2\text{Yb}_2\text{Me}_2(\text{OH})_2\text{Li}_2(\text{TMEDA})_2 \cdot (\text{Et}_2\text{O})$  (**16**) (ellipsoids are drawn at the 50% probability level; all hydrogen atoms are omitted for clarity).

Unexpectedly, the reaction of  $[\text{Li}(\text{TMEDA})][\text{YbMe}_4]$  with  $\{\text{LON}^{\text{iPr}}\}_2\text{H}_2$ , carried out under conditions identical to those used for other elements (Scheme 10), led to the isolation in 67% yield of  $\{\text{LON}^{\text{iPr}}\}_2\text{Yb}_2\text{Me}_2(\text{OH})_2\text{Li}_2(\text{TMEDA})_2$  (**16**) as pale-yellow crystals (Scheme 11). Suitable crystals of **16** were studied by X-ray crystallography (Figure 10). The molecule of **16** is very similar to those of **12** and **13**, exhibiting the same organization of the coordination spheres at the ytterbium and lithium centers. The presence of adventitious water and the extreme sensitivity of the putative intermediate  $\{\text{LON}^{\text{iPr}}\}_2\text{Yb}_2\text{Me}_4\text{Li}_2(\text{TMEDA})_2$  are the most probable reasons that can be envisioned for the origin of the OH ligands in this compound.

It is worth noting that the multidentate coordination of phenoxy-amidate ligands in the amido and dimethyl complexes gives rise to the formation of dimeric chiral molecules that feature cis/trans stereoisomerism (Scheme 12). For instance, complexes **6**, **9**, **13**, and **16** were found to adopt a  $C_2$ -symmetric cis configuration in the solid state. They can be regarded as cis heterochiral dimeric molecules according to the existing classification.<sup>27</sup> On the other hand, **12** adopts in the solid state a  $C_2$ -symmetric homochiral trans form. These differences may be accounted for by possible dynamic interconversion processes between the cis and trans forms of these dimeric molecules. Such a process is apparently fairly rapid on the NMR time scale, as shown by the completely symmetric sets of signals in the NMR spectra of dimeric diamagnetic complexes **6**, **12**, and **16** (vide supra).

**Scheme 12.** *cis* and *trans* Isomerism in Dimeric Phenoxy-Amidinate Complexes **6**, **9**, **13**, and **16**, and Interconversion Processes



**Ring-Opening Polymerization Studies.** We next evaluated the performances of the prepared compounds  $\{LON^R\}Ln(N;SiMe_3)_2$  that possess a potentially reactive nucleophilic amido group, that is, **6**, **8**, and **9**, as initiators/catalysts in the ROP of *racemic* lactide (*rac*-LA) (Scheme 13).<sup>28</sup> Representative results are summarized in Table 3.

Use of these amido complexes as initiators (i.e., in the absence of any external co-initiator, *vide infra*) revealed they are moderately active at room temperature. Compounds **6** and **8**, which incorporate, respectively, isopropyl and cyclohexyl substituents at amidinate groups, featured similar activities equally in THF and toluene solvents. Also, the yttrium and neodymium compounds **8** and **9** displayed about the same activities. Interestingly, the homodecoupled <sup>1</sup>H NMR spectra of the PLAs formed showed significantly heterotactic-enriched microstructures. The  $P_r$  (probability of racemic linkage) values were in the range of 0.64–0.76, depending on the nature of the initiator and solvent. The PLA samples obtained under these conditions (i.e., in the absence of any external co-initiator) all had monomodal, but broad, molecular weight distributions ( $M_w/M_n = 1.5–2.6$ ). The relatively poor degree of control provided by these systems in terms of molecular weights is also illustrated by the experimental  $M_n$  values that were quite often significantly higher than the theoretical ones; a noticeable exception is the good match observed between  $M_{n,calc}$  and  $M_{n,exptl}$  values for polymers prepared from **6** in THF (Table 3, entries 5 and 6). Both features—relatively high

polydispersity and molecular weights values—are indicative of relatively slow initiation as compared to chain-propagation reaction. It must be noted that this general trend was observed with rare-earth amido complexes in the ROP of lactide.<sup>3–5</sup>

On the other hand, the ROP of *rac*-LA proceeded in a much better controlled fashion when alcohols (i.e., *i*PrOH or PhCH<sub>2</sub>OH) were added in the reaction medium as external co-initiator/chain transfer agents (Table 3, entries 14–22). For instance, the ROP of 500–1000 equiv of *rac*-LA was performed using **6** in the presence of 5–50 equiv (vs Y) of *i*PrOH, eventually yielding PLAs with accordingly decreased molecular weights. The much narrower polydispersities ( $M_w/M_n = 1.11–1.34$ ) observed under those conditions, as compared with those obtained without alcohol added, and the good match between calculated and experimental molecular weights argue for fast and reversible transfer reactions. <sup>1</sup>H NMR spectroscopic analysis of the low-molecular-weight PLA produced with 50 equiv of *i*PrOH under such conditions (entry 19) was in agreement with selective capping of the PLA chains with *i*PrOC(O)– and HOCH(CH<sub>3</sub>)CO– end-groups, thus supporting the transfer process of an effective immortal polymerization.<sup>29</sup> However, under those immortal conditions, the catalyst systems were not stereoselective any longer as essentially atactic PLAs were recovered.

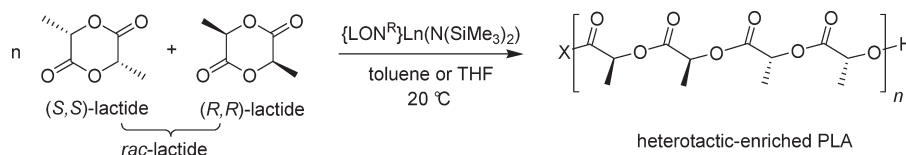
## CONCLUSIONS

We have prepared new multidentate ligand systems combining phenoxy and amidinate fragments into a dianionic chelating platform. These systems have been successfully used to prepare phenoxy-amidinate complexes of group 3 and lanthanide metals. Ligands with relatively less sterically demanding isopropyl and cyclohexyl *N,N'*-disubstituted amidinate fragments lead to dimeric complexes, whereas the bulkier di(2,6-isopropyl)phenyl *N,N'*-disubstituted version of this ligand system apparently favors the formation of monomeric complexes in which the ligand acts as a monoanionic phenoxy-amidinate. Dimeric complexes of isopropyl and cyclohexyl *N,N'*-disubstituted ligands exhibit stereoselective coordination onto the metal centers, giving rise to *cis/trans* isomerism. These isomers have been identified in the solid state by X-ray diffraction studies, and they rapidly interconvert in solution, as observed by NMR spectroscopy. Amido complexes of these phenoxy-amidinate ligands are active initiators or catalysts, when combined with *i*PrOH or PhCH<sub>2</sub>OH used as co-initiators/chain transfer agents, in the ROP of *racemic* lactide, giving atactic to heterotactic-enriched PLAs.

## EXPERIMENTAL SECTION

**General Conditions.** All manipulations requiring an anhydrous atmosphere were performed under a purified argon atmosphere using standard Schlenk techniques or in a glovebox. Anhydrous LnCl<sub>3</sub> precursors (99.99%) were purchased from Strem Chemicals and used as received. TMEDA was purchased from Acros and dried over 3A molecular sieves before use. The metal precursors, Ln(N(SiMe<sub>3</sub>)<sub>2</sub>·(Et<sub>2</sub>O))<sub>3</sub>,<sup>30</sup> Ln[N(SiMe<sub>3</sub>)<sub>2</sub>]<sub>3</sub>,<sup>31</sup> and [Li(TMEDA)][LnMe<sub>4</sub>]<sub>2</sub><sup>5b</sup> were prepared by the corresponding literature procedures. Solvents were freshly distilled from Na/benzophenone (THF, toluene, Et<sub>2</sub>O, DME) or Na/K amalgam (pentane, hexanes) under argon and degassed thoroughly by freeze–pump–thaw cycles prior to use. Deuterated solvents (THF-*d*<sub>8</sub>, benzene-*d*<sub>6</sub>, toluene-*d*<sub>8</sub>, pyridine-*d*<sub>5</sub>) were freshly distilled from Na/K amalgam under argon and degassed prior to use. *Racemic* lactide (Aldrich) was recrystallized from *i*PrOH and twice from dry

Scheme 13


**Table 3. Ring-Opening Polymerization of *racemic* Lactide Promoted by Amido Phenoxy-Amidinate Rare-Earth Complexes {LON<sup>R</sup>}LnN(SiMe<sub>3</sub>)<sub>2</sub><sup>a</sup>**

entry	comp.	ROH	[LA]/[Ln]/[ROH]	solvent	time (min) <sup>b</sup>	conv (%) <sup>c</sup>	$M_{n,calc}^d/10^3 \text{ g mol}^{-1}$	$M_{n,exptl}^e/10^3 \text{ g mol}^{-1}$	$M_w/M_n^e$	$P_r^{f,g}$
1	6		100:1:0	toluene	25	10	1.44	14.33	1.5 <sub>4</sub>	nd
2	6		100:1:0	toluene	80	83	12.00	28.42	2.6 <sub>3</sub>	nd
3	6		100:1:0	toluene	240	98	14.11	20.02	1.9 <sub>1</sub>	0.68
4	6		100:1:0	toluene	720	99	14.90	23.54	2.2 <sub>4</sub>	nd
5	6		100:1:0	THF	240	96	13.82	15.50	2.2 <sub>3</sub>	0.69
6	6		100:1:0	THF	720	98	14.11	16.24	2.0 <sub>1</sub>	nd
7	8		100:1:0	toluene	720	99	14.26	23.58	2.6 <sub>0</sub>	0.64
8	8		100:1:0	THF	720	98	14.11	24.40	2.5 <sub>5</sub>	0.76
9	9		100:1:0	toluene	120	30	4.32	8.26	1.5 <sub>0</sub>	nd
10	9		100:1:0	toluene	720	100	14.40	49.00	1.6 <sub>0</sub>	nd
11	9		100:1:0	THF	720	99	14.26	58.12	1.7 <sub>1</sub>	0.72
12	9		350:1:0	toluene	840	79	38.68	105.20	1.6 <sub>8</sub>	nd
13	9		500:1:0	toluene	1500	74	53.28	158.77	1.7 <sub>6</sub>	0.67
14	6	PhCH <sub>2</sub> OH	100:1:5	toluene	80	20	0.58	0.33	1.2 <sub>7</sub>	nd
15	6	PhCH <sub>2</sub> OH	100:1:5	toluene	180	95	2.70	1.51	1.2 <sub>0</sub>	0.50
16	6	<i>i</i> PrOH	100:1:5	toluene	80	53	1.53	1.31	1.2 <sub>0</sub>	nd
17	6	<i>i</i> PrOH	100:1:5	toluene	180	94	2.70	1.64	1.1 <sub>9</sub>	0.50
18	6	<i>i</i> PrOH	500:1:5	toluene	240	63	9.07	5.52	1.1 <sub>1</sub>	0.52
19	6	<i>i</i> PrOH	500:1:50	toluene	240	70	1.01	0.82 (1.04) <sup>f</sup>	1.2 <sub>5</sub>	0.50
20	6	<i>i</i> PrOH	1000:1:5	toluene	720	25	7.21	6.83	1.1 <sub>3</sub>	nd
21	6	<i>i</i> PrOH	1000:1:5	toluene	1800	100	28.80	23.78	1.3 <sub>4</sub>	0.52
22	9	<i>i</i> PrOH	100:1:5	toluene	120	100	2.88	2.36	1.3 <sub>8</sub>	nd

<sup>a</sup> General conditions: [*rac*-LA] = 1.0 mol L<sup>-1</sup>, T = 20 °C, unless otherwise stated. <sup>b</sup> Reactions times were not optimized. <sup>c</sup> Conversion of lactide as determined by <sup>1</sup>H NMR on the crude reaction mixture. <sup>d</sup>  $M_n$  values calculated considering one polymer chain per metal center from the relation:  $M_{n,calc} = \text{Conv.} \times [\text{LA}]/[\text{Ln}] \times 144$ . <sup>e</sup> Experimental  $M_n$  and  $M_w/M_n$  values determined by GPC in THF vs PS standards and corrected with a factor of 0.58. <sup>f</sup> Determined by <sup>1</sup>H NMR. <sup>g</sup>  $P_r$  is the probability of racemic linkage, as determined by <sup>1</sup>H NMR homodecoupling experiments.

toluene, and dried in vacuum. Other starting materials were purchased from Acros, Strem, and Aldrich and used as received.

**Instruments and Measurements.** NMR spectra were recorded on Bruker AC 200, Bruker ACP 200, Bruker AC 300, Bruker Avance DRX 400, and Bruker AC 500 spectrometers in Teflon-valved NMR tubes. <sup>1</sup>H and <sup>13</sup>C NMR chemical shifts are reported in parts per million versus SiMe<sub>4</sub> and were determined by reference to the residual solvent resonances. Assignment of signals was carried out via multinuclear 1D (<sup>1</sup>H, <sup>13</sup>C{<sup>1</sup>H}) and 2D (<sup>1</sup>H–<sup>13</sup>C HMBC and HMQC) NMR experiments. Coupling constants are reported in hertz. <sup>7</sup>Li NMR chemical shifts are reported versus LiCl(aq).

C, H, and N elemental analyses were performed by the microanalytical laboratory of IOMC. Lanthanide metal analysis was carried out by complexometric titration. IR spectra were recorded either as Nujol mulls or using ATR module on a Bruker-Vertex 70 spectrophotometer.

Size exclusion chromatography (SEC) of PLAs was performed in THF (1 mL min<sup>-1</sup>) at 20 °C using a Polymer Laboratories PL50 apparatus equipped with PLgel 5 μm MIXED-C 300 × 7.5 mm columns, and combined RI and Dual angle LS (PL-LS 45/90°) detectors. The number-average molecular masses ( $M_n$ ) and polydispersity index

( $M_w/M_n$ ) of the polymers were calculated with reference to a universal calibration versus polystyrene standards. The  $M_n$  values of PLAs were corrected with a factor of 0.58 to account for the difference in hydrodynamic volumes between polystyrene and polylactide.<sup>46,32</sup> The microstructure of PLAs was determined by homodecoupling <sup>1</sup>H NMR spectroscopy at 25 °C in CDCl<sub>3</sub> with a Bruker AC-500 spectrometer operating at 500 MHz.

{(*i*PrN)<sub>2</sub>CC<sub>6</sub>H<sub>2</sub>(*t*Bu)<sub>2</sub>O}H<sub>2</sub> ({LON<sup>*i*Pr</sup>}H<sub>2</sub>). To a solution of 2-bromo-4,6-(di-*tert*-butyl)phenol (3.90 g, 13.67 mmol) in diethyl ether (30 mL) was added *n*-butyllithium (11.48 mL of a 2.50 M solution in hexane, 28.71 mmol) at 0 °C. The reaction mixture was stirred for 0.5 h at room temperature and a solution of *N,N'*-diisopropylcarbodiimide (2.23 mL, 14.31 mmol) in diethyl ether (10 mL) was added dropwise. The reaction mixture was stirred under reflux overnight and then cooled to room temperature. The white precipitate formed was separated by filtration under argon. Water (50 mL) and Et<sub>2</sub>O (50 mL) were added stepwise. The organic layer was separated and dried over NaSO<sub>4</sub>, and volatiles were removed in vacuo. The residue was dried in vacuo to give {LON<sup>*i*Pr</sup>}H<sub>2</sub> as a pale yellow solid (3.82 g, 11.48 mmol, 84%). mp = 158 °C. <sup>1</sup>H NMR (CDCl<sub>3</sub>, 500 MHz, 25 °C): δ 7.35 (d, J = 2.5, 1H,

$C_6H_2$ ), 7.30 (s, 1H,  $C_6H_2$ ), 3.78 (hept,  $J = 6.3$ , 2H,  $CH(CH_3)$ ), 1.48 (s, 9H,  $C(CH_3)_3$ ), 1.34 (s, 9H,  $C(CH_3)_3$ ), 1.16 (d,  $J = 6.3$ , 12H,  $CH(CH_3)_2$ ).  $^{13}C\{^1H\}$  NMR ( $CDCl_3$ , 125 MHz, 25 °C):  $\delta$  160.8 ( $CN_2$ ), 159.1 ( $O-C_6H_2$ ), 137.3, 137.5, 125.9, 122.5, 114.7, 47.2 ( $CH(CH_3)_2$ ), 35.2 ( $Ph-C(CH_3)_3$ ), 34.2 ( $Ph-C(CH_3)_3$ ), 31.6 ( $Ph-C(CH_3)_3$ ), 29.7 ( $Ph-C(CH_3)_3$ ), 24.3 ( $CH(CH_3)_2$ ). Anal. Calcd for  $C_{21}H_{36}N_2O$ : C, 75.85; H, 10.91; N, 8.42. Found: C, 75.34; H, 10.25; N, 8.35.

$\{(CyN)_2CC_6H_2(tBu)_2O\}H_2$  ( $\{LON^{Cy}\}H_2$ ). A protocol similar to that described above for **1-H** was used, starting from 2-bromo-4,6-(di-*tert*-butyl)phenol (7.87 g, 27.6 mmol), *n*-butyllithium (23.20 mL of a 2.50 M solution in hexane, 57.9 mmol), and *N,N'*-dicyclohexylcarbodiimide (5.98 g, 29.0 mmol). Workup afforded  $\{LON^{Cy}\}H_2$  as a yellowish solid (9.79 g, 23.7 mmol, 86%). mp = 121 °C.  $^1H$  NMR ( $CDCl_3$ , 500 MHz, 25 °C):  $\delta$  7.35 (d,  $J = 2.5$ , 1H,  $C_6H_2$ ), 7.31 (d,  $J = 2.5$ , 1H,  $C_6H_2$ ), 3.45 (br m, 2H,  $CH(CH_2)$ , Cy), 1.99 (br m, 4H, Cy), 1.81 (br m, 4H, Cy), 1.67 (br m, 2H, Cy), 1.49 (s, 9H,  $C(CH_3)_3$ ), 1.35 (br m, 10H, Cy), 1.34 (s, 9H,  $C(CH_3)_3$ ).  $^{13}C\{^1H\}$  NMR ( $CDCl_3$ , 125 MHz, 25 °C):  $\delta$  160.9 ( $CN_2$ ), 160.6 ( $O-C_6H_2$ ), 137.8, 136.9, 126.0, 122.2, 113.9, 54.7 ( $NCH(CH_2)_5$ ), 35.2 ( $Ph-C(CH_3)_3$ ), 34.8 ( $CH(CH_2)_5$ ), 34.2 ( $Ph-C(CH_3)_3$ ), 31.6 ( $Ph-C(CH_3)_3$ ), 29.6 ( $Ph-C(CH_3)_3$ ), 25.5 ( $CH(CH_2)_5$ ), 25.0 ( $CH(CH_2)_5$ ). Anal. Calcd for  $C_{27}H_{44}N_2O$ : C, 78.59; H, 10.75; N, 6.79. Found: C, 78.16; H, 10.56; N, 6.55.

$\{(iPr)_2C_6H_3N)_2CC_6H_2(tBu)_2O\}H_2$  ( $\{LON^{iPr}\}H_2$ ). A protocol similar to that described above for  $\{LON^{iPr}\}H_2$  was used, starting from 2-bromo-4,6-di(*tert*-butyl)phenol (15.7 g, 55.0 mmol), *n*-butyllithium (46.2 mL of a 2.50 M solution in hexane, 115.6 mmol), and *N,N'*-di(bis-2,6-diisopropylphenyl)carbodiimide (20.95 g, 57.8 mmol). Workup afforded  $\{LON^{iPr}\}H_2$  as a yellowish oil. The latter was purified by removing volatiles in vacuo using a Kugelrohr apparatus ( $2 \times 10^{-2}$  Torr, 120 °C) to afford a brownish solid (9.85 g, 17.3 mmol, 31%). mp = 151 °C.  $^1H$  NMR ( $CD_2Cl_2$ , 500 MHz, 25 °C):  $\delta$  7.30–7.18 (m, 6H,  $C_6H_2$ ), 7.10 (m, 2H,  $C_6H_2$ ), 6.67 (d,  $J = 2.4$ , 1H, OH or NH), 5.89 (s, 1H, OH or NH), 3.25 (hept,  $J = 6.7$ , 2H,  $CH(CH_3)$ ), 3.06 (hept,  $J = 6.7$ , 2H,  $CH(CH_3)$ ), 1.50 (s, 9H,  $C(CH_3)_3$ ), 1.36 (d,  $J = 6.7$ , 6H,  $CH(CH_3)$ ), 1.24 (d,  $J = 6.7$ , 6H,  $CH(CH_3)$ ), 1.06 (d,  $J = 6.7$ , 6H,  $CH(CH_3)$ ), 0.90 (s, 9H,  $C(CH_3)_3$ ), 0.87 (d,  $J = 6.7$ , 6H,  $CH(CH_3)$ ).  $^{13}C\{^1H\}$  NMR ( $CDCl_3$ , 75 MHz, 25 °C):  $\delta$  158.0 ( $CN_2$ ), 156.5 ( $O-C_6H_2$ ), 144.6, 140.8, 137.2, 135.0, 126.2, 124.3, 124.1, 123.4, 112.7, 35.3 ( $Ph-C(CH_3)_3$ ), 33.8 ( $Ph-C(CH_3)_3$ ), 31.2 ( $Ph-C(CH_3)_3$ ), 29.6 ( $Ph-C(CH_3)_3$ ), 24.9 ( $Ph-CH(CH_3)_2$ ), 24.8 ( $Ph-CH(CH_3)_2$ ), 22.3 ( $Ph-CH(CH_3)_2$ ), 22.1 ( $Ph-CH(CH_3)_2$ ). Anal. Calcd for  $C_{27}H_{44}N_2O$ : C, 82.34; H, 9.92; N, 4.92. Found: C, 82.88; H, 10.05; N, 4.89.

$\{(iPr)_2C_6H_3N)_2CC_6H_2(tBu)_2O\}Li_2$  ( $\{LON^{iPr}\}Li_2(Et_2O)_{0.5}$ , **1**). To a solution of  $\{LON^{iPr}\}H_2$  (2.00 g, 6.02 mmol) in diethyl ether (20 mL) was added *n*-butyllithium (4.81 mL of a 2.50 M solution in hexane, 12.04 mmol) at 0 °C under stirring. The resulting yellowish reaction mixture was stirred at room temperature overnight. Volatiles were then evaporated in vacuo to give **1** as a white powder (2.25 g, 5.89 mmol, 98%). Crystals of  $[\{LON^{iPr}\}Li_2(THF)_2]_2 \cdot (THF)$  suitable for X-ray diffraction studies were obtained from a THF/hexane (1:1 v/v) solution.  $^1H$  NMR (THF- $d_8$ , 500 MHz, 25 °C):  $\delta$  7.35 (s, 1H,  $C_6H_2$ ), 6.60 (s, 1H,  $C_6H_2$ ), 3.38 (q,  $J = 7.0$ , 2H,  $OCH_2CH_3$ ), 3.15 (br m, 2H,  $CH(CH_3)$ ), 1.45 (br s, 9H,  $C(CH_3)_3$ ), 1.24 (br s, 9H,  $C(CH_3)_3$ ), 1.11 (t,  $J = 7.0$ , 2H,  $OCH_2CH_3$ ), 0.84 (br m, 12H,  $CH(CH_3)_2$ ).  $^{13}C\{^1H\}$  NMR (THF- $d_8$ , 125 MHz, 25 °C):  $\delta$  176.8 ( $CN_2$ ), 158.6 ( $O-C_6H_2$ ), 132.9, 129.2, 125.9, 120.9, 118.5, 118.4, 63.5 ( $CH_2$ ,  $Et_2O$ ), 44.8 ( $CH(CH_3)_2$ ), 31.9 ( $Ph-C(CH_3)_3$ ), 31.5 ( $Ph-C(CH_3)_3$ ), 29.7 ( $Ph-C(CH_3)_3$ ), 28.2 ( $Ph-C(CH_3)_3$ ), 24.9 ( $CH(CH_3)_2$ ), 24.7 ( $CH(CH_3)_2$ ), 12.8 ( $CH_3$ ,  $Et_2O$ ). Anal. Calcd for  $C_{92}H_{156}Li_8N_8O_6$ : C, 72.42; H, 10.71; N, 7.34. Found: C, 72.16; H, 10.56; N, 7.26.

$\{(iPr)_2C_6H_3N)_2CC_6H_2(tBu)_2O\}Li_2$  ( $\{LON^{Ar}\}Li_2$ , **2**). A protocol similar to that described above for **1** was used, starting from  $\{LON^{Ar}\}H_2$  (1.50 g, 2.64 mmol) and *n*-butyllithium (2.11 mL of a 2.50 M solution in

hexane, 5.28 mmol). Workup afforded **2** as an off-white solid (2.11 g, 3.63 mmol, 98%). Crystals of  $\{LON^{Ar}\}Li_2(THF)_3$  suitable for X-ray diffraction studies were obtained from a THF/hexane (1:1 v/v) solution at room temperature.  $^1H$  NMR (THF- $d_8$ , 500 MHz, 25 °C):  $\delta$  6.99 (br m, 2H, arom), 6.87 (br m, 2H, Ar), 6.67 (br m, 2H, arom), 6.55–6.45 (br m, 2H, arom), 3.33 (br m, 2H,  $CH(CH_3)$ ), 3.00 (br m, 2H,  $CH(CH_3)$ ), 1.45 (s, 9H,  $C(CH_3)_3$ ), 1.21 (br m, 6H,  $CH(CH_3)_2$ ), 1.15 (br m, 6H,  $CH(CH_3)_2$ ), 0.80 (s, 9H,  $C(CH_3)_3$ ), 0.77 (br s, 6H,  $CH(CH_3)_2$ ), 0.64 (br s, 6H,  $CH(CH_3)_2$ ).  $^{13}C\{^1H\}$  NMR (THF- $d_8$ , 125 MHz, 25 °C):  $\delta$  160.9 ( $CN_2$ ), 160.2 ( $O-C_6H_2$ ), 148.2, 141.2, 135.8, 135.5, 129.9, 124.6, 119.8, 119.5, 119.0, 115.3, 39.5 ( $Ph-C(CH_3)_3$ ), 33.2 ( $Ph-C(CH_3)_3$ ), 31.3 ( $Ph-C(CH_3)_3$ ), 29.3 ( $Ph-CH(CH_3)_2$ ), 27.7 ( $Ph-C(CH_3)_3$ ), 26.8 ( $Ph-CH(CH_3)_2$ ), 25.8 ( $Ph-CH(CH_3)_2$ ), 23.5 ( $Ph-CH(CH_3)_2$ ), 22.9 ( $Ph-CH(CH_3)_2$ ), 20.3 ( $Ph-CH(CH_3)_2$ ). Anal. Calcd for  $C_{39}H_{54}Li_2N_2O$ : C, 80.66; H, 9.37; N, 4.95. Found: C, 80.45; H, 9.43; N, 4.55.

$\{(iPr)_2C_6H_3N)_2CC_6H_2(tBu)_2O\}YCl_2$  ( $\{LON^{iPr}\}YCl_2$ , **3**). To a solution of  $\{LON^{iPr}\}H_2$  (0.92 g, 2.78 mmol) in toluene (10 mL) was added *n*-butyllithium (6.0 mL of a 0.93 M solution in hexane, 5.56 mmol) at 0 °C, and the reaction mixture was stirred during 20 min at 0 °C and then during 30 min at room temperature. Volatiles were evaporated in vacuo, the solid residue was dissolved in THF (10 mL), and the solution was added to a suspension of yttrium chloride (0.54 g, 2.78 mmol) in THF (10 mL) at room temperature. The reaction mixture was stirred during 12 h. THF was evaporated in vacuo, and the solid residue was extracted with toluene (20 mL). The clear solution was concentrated at 0 °C to afford **3** (0.70 g, 1.54 mmol, 56%) as a white crystalline powder.  $^1H$  NMR (THF- $d_8$ , 500 MHz, 25 °C):  $\delta$  7.29 (br s, 2H,  $C_6H_2$ ), 7.06 (br s, 2H,  $C_6H_2$ ), 3.48 (br sept, 4H,  $CH(CH_3)_2$ ), 1.48 (br s, 18H,  $C(CH_3)_3$ ), 1.29 (br s, 18H,  $C(CH_3)_3$  that overlapped with 12H,  $CH(CH_3)_2$ ), 1.21 (br s, 12,  $CH(CH_3)_2$ ).  $^{13}C\{^1H\}$  NMR (THF- $d_8$ , 125 MHz, 25 °C):  $\delta$  184.8 ( $CN_2$ ), 163.7 ( $O-C_6H_2$ ), 137.5 ( $C_6H_2tBu$ ), 136.5 ( $C_6H_2-tBu$ ), 125.1 ( $C_6H_2$ ), 123.4 ( $C_6H_2$ ), 122.4 ( $C_6H_2$ ), 46.9 ( $CH(CH_3)_2$ ), 33.0 ( $Ph-C(CH_3)_3$ ), 31.8 ( $Ph-C(CH_3)_3$ ), 29.3 ( $CH(CH_3)_2$ ), 27.3 ( $Ph-C(CH_3)_3$ ), 24.1 ( $Ph-C(CH_3)_3$ ). IR (Nujol, KBr)  $\nu$  ( $cm^{-1}$ ): 1609 s, 1571 s, 1530 w, 1366 m, 1294 w, 1259 m, 1226 m, 1200 w, 1181 w, 1168 w, 1146 w, 1128 w, 1119 w, 1073 w, 1049 m, 1032 m, 963 w, 918 w, 888 m, 844 s, 786 m, 757 w, 646 w, 614 m, 530 m. Anal. Calcd for  $C_{42}H_{68}Cl_2N_4O_2Y_2$ : C, 55.45; H, 7.53; N, 6.16; Y, 19.55. Found: C, 55.80; H, 7.72; N, 6.31; Y, 19.65.

$\{(iPr)_2C_6H_3N)_2(H)CC_6H_2(tBu)_2O\}YCl_2 \cdot DME$  ( $\{LO^{HAr}\}YCl_2 \cdot (DME)$ , **5**). To a solution of  $\{LO^{HAr}\}H_2$  (0.33 g, 0.578 mmol) in hexanes (10 mL) was added *n*-butyllithium (1.0 mL of a 1.16 M solution in hexane, 1.16 mmol) at 0 °C. The reaction mixture was stirred during 20 min at 0 °C and then during 30 min at room temperature. Volatiles were evaporated in vacuo, the solid residue was dissolved in THF (10 mL), and the solution was added to a suspension of yttrium chloride (0.133 g, 0.578 mmol) in THF (10 mL) at room temperature. The reaction mixture was stirred during 24 h. THF was evaporated in vacuo, and the solid residue was extracted with toluene (20 mL). Toluene was evaporated, and the residue was dissolved in a DME/hexane (1:10 v/v) mixture. The clear solution was concentrated at 0 °C to afford **5** as a white crystalline powder (0.15 g, 32%). Colorless crystals suitable for X-ray diffraction studies were obtained by slow concentration of a solution in a DME/hexane (1:10 v/v) mixture at room temperature.  $^1H$  NMR ( $C_6D_6$ , 500 MHz, 60 °C):  $\delta$  7.36 (d,  $^4J = 2.5$ , 1H,  $C_6H_2$ ), 7.27 (d,  $^3J = 7.5$ , 2H,  $C_6H_3$ ), 7.17 (t,  $^3J = 7.5$ , 1H,  $C_6H_3$ ), 7.11 (d,  $^3J = 7.5$ , 2H,  $C_6H_3$ ), 7.07 (d,  $^4J = 2.5$ , 1H,  $C_6H_2$ ), 6.92 (t,  $^3J = 7.5$ , 1H,  $C_6H_3$ ), 3.88 (br sept, 2H,  $CH(CH_3)_2$ ), 3.33 (br sept, 2H,  $CH(CH_3)_2$ ), 3.14 (br s, 6H,  $(CH_3)_2$  DME), 3.10 (br s, 4H,  $CH_2$ , DME), 1.78 (br s, 9H,  $C(CH_3)_3$ ), 1.51 (d,  $^3J = 6.4$ , 6H,  $CH(CH_3)_2$ ), 1.44 (d,  $^3J = 6.4$ , 6H,  $CH(CH_3)_2$ ), 1.14 (br s, 9H,  $C(CH_3)_3$  overlapped with 6H of  $CH(CH_3)_2$ ), 1.03 (d,  $^3J = 6.4$ , 6H,  $CH(CH_3)_2$ ).  $^{13}C\{^1H\}$  NMR ( $C_6D_6$ , 125 MHz, 25 °C):  $\delta$  162.3 ( $CN_2$ ), 157.0 ( $O-C_6H_2$ ), 146.8 ( $C_6H_3-iPr$ ), 137.6 ( $C_6H_2-tBu$ ),

127.8 ( $C_6H_2$ ), 126.2 ( $N-C_6H_3$ ), 123.8 ( $C_6H_3$ ), 122.8 ( $C_6H_3$ ), 122.5 ( $C_6H_2$ ), 119.6 ( $C_6H_3$ ), 71.0 ( $CH_2$ , DME), 59.1 ( $CH_3$ , DME), 35.2 ( $Ph-C(CH_3)_3$ ), 33.8 ( $Ph-C(CH_3)_3$ ), 31.4 ( $Ph-C(CH_3)_3$ ), 30.6 ( $Ph-C(CH_3)_3$ ), 28.7 ( $Ph-CH(CH_3)_2$ ), 27.9 ( $Ph-CH(CH_3)_2$ ), 26.6 ( $Ph-CH(CH_3)_2$ ), 24.5 ( $Ph-CH(CH_3)_2$ ), 22.8 ( $Ph-CH(CH_3)_2$ ). IR (Nujol, KBr)  $\nu$  ( $cm^{-1}$ ): 3341 w, 3171 w, 1600 m, 1544 s, 1189 m, 1080 s, 1036 s, 968 m, 859 s, 780 m, 766 m. Anal. Calcd for  $C_{43}H_{65}Cl_2N_2O_3Y$ : C, 63.15; H, 8.01; N, 3.43; Y, 10.87. Found: C, 62.93; H, 8.11; N, 3.67; Y, 10.80.

**[{(iPrN)<sub>2</sub>CC<sub>6</sub>H<sub>2</sub>(tBu)<sub>2</sub>O<sub>2</sub>Y(N(SiMe<sub>3</sub>)<sub>2</sub>)<sub>2</sub>}{LON<sup>Pr</sup>}Y(N(SiMe<sub>3</sub>)<sub>2</sub>), 6].**  
*Method A.* To a solution of **3** (0.67 g, 2.78 mmol) in THF (10 mL) was added a solution of Na[N(SiMe<sub>3</sub>)<sub>2</sub>] (0.27 g, 2.78 mmol) in THF (10 mL) at room temperature, and the reaction mixture was stirred during 48 h. Volatiles were evaporated in vacuo, and the solid residue was extracted with hexanes (30 mL). Hexanes were evaporated, and the solid residue was dried in vacuo during 12 h to afford **6** as a pale yellow crystalline powder (0.64 g, 1.09 mmol, 74%). Crystals suitable for X-ray diffraction studies were obtained from a Et<sub>2</sub>O solution at room temperature.

*Method B.* To a solution of {LON<sup>Pr</sup>}H<sub>2</sub> (0.303 g, 0.91 mmol) in toluene (10 mL) was added *n*-butyllithium (1.33 mL of a 1.37 M solution in hexane, 1.82 mmol) at 0 °C, and the reaction mixture was stirred during 20 min at 0 °C and then during 30 min at room temperature. Volatiles were evaporated in vacuo, the solid residue was redissolved in THF (10 mL), and the resulting solution was then added to a suspension of yttrium chloride (0.178 g, 0.91 mmol) in THF (10 mL) at room temperature. The reaction mixture was stirred during 12 h, and a solution of Li[N(SiMe<sub>3</sub>)<sub>2</sub>]·Et<sub>2</sub>O (0.219 g, 0.91 mmol) in THF (10 mL) was added in at room temperature. The reaction mixture was stirred during 12 h, and then volatiles were evaporated in vacuo. The solid residue was extracted with hexanes (30 mL), and the clear solution was concentrated at 0 °C to afford **6** as a white crystalline powder (0.410 g, 0.354 mmol, 78%). <sup>1</sup>H NMR ( $C_6D_6$ , 400 MHz, 25 °C):  $\delta$  7.57 (br s, 2H,  $C_6H_2$ ), 7.16 (br s, 2H,  $C_6H_2$ ), 3.65 (br m, 4H,  $CH(CH_3)_2$ ), 1.66 (s, 18H,  $C(CH_3)_3$ ), 1.34 (s, 18H,  $C(CH_3)_3$ ), 1.24 (br m, 24H,  $CH(CH_3)_2$ ), 0.46 (br s, 36H, N(Si(CH<sub>3</sub>)<sub>3</sub>)<sub>2</sub>). <sup>13</sup>C{<sup>1</sup>H} NMR ( $C_6D_6$ , 100 MHz, 25 °C):  $\delta$  187.0 (CN<sub>2</sub>), 161.3 (O- $C_6H_2$ ), 137.5 ( $C_6H_2$ -tBu), 137.2 ( $C_6H_2$ -tBu), 125.5 ( $C_6H_2$ ), 124.0 ( $C_6H_2$ -CN<sub>2</sub>), 122.5 ( $C_6H_2$ ), 49.4 ( $CH(CH_3)_2$ ), 35.3 ( $Ph-C(CH_3)_3$ ), 33.9 ( $Ph-C(CH_3)_3$ ), 31.6 ( $Ph-C(CH_3)_3$ ), 29.5 ( $Ph-C(CH_3)_3$ ), 24.6 ( $CH(CH_3)_2$ ), 5.3 (N(Si(CH<sub>3</sub>)<sub>3</sub>)<sub>2</sub>). IR (Nujol, KBr)  $\nu$  ( $cm^{-1}$ ): 1600 s, 1546 w, 1508 s, 1437 s, 1408 m, 1365 m, 1288 s, 1259 w, 1246 m, 1223 m, 1194 m, 1171 m, 1147 s, 1126 s, 1094 w, 1026 m, 1015 w, 967 s, 872 s, 842 s, 829 m, 779 m, 756 s, 695 w, 667 s, 617 s, 597 m, 572 w, 549 s, 529 m. Anal. Calcd for  $C_{54}H_{104}N_6O_2Si_4Y_2$ : C, 55.93; H, 9.04; N, 7.25; Y, 15.33. Found: C, 56.05; H, 9.08; N, 7.14; Y, 15.10.

*Method C.* In the glovebox, a Teflon-valved NMR tube was charged with {LON<sup>Pr</sup>}H<sub>2</sub> (0.012 g, 0.036 mmol) and Y[N(SiMe<sub>3</sub>)<sub>2</sub>]<sub>3</sub> (0.0206 g, 0.036 mmol). To this mixture was transferred in THF-*d*<sub>8</sub> (ca. 0.6 mL) under vacuum, and the tube was sealed. The tube was shaken over 48 h before NMR was recorded, after which time period the quantitative formation of **6** was observed. <sup>1</sup>H NMR (THF-*d*<sub>8</sub>, 200 MHz, 25 °C):  $\delta$  7.09 (d, <sup>4</sup>J = 2.2, 2H,  $C_6H_2$ ), 6.93 (d, <sup>4</sup>J = 2.2, 2H,  $C_6H_2$ ), 3.08 (sept, <sup>3</sup>J = 6.2, 4H,  $CH(CH_3)_2$ ), 1.40 (s, 18H,  $C(CH_3)_3$ ), 1.28 (s, 18H,  $C(CH_3)_3$ ), 1.01 (d, <sup>3</sup>J = 6.2, 24H,  $CH(CH_3)_2$ ), 0.17 (br s, 36H, N(Si(CH<sub>3</sub>)<sub>3</sub>)<sub>2</sub>).

**Synthesis of {LON<sup>Ar</sup>}<sub>2</sub>YLi(THF)<sub>2</sub> (**7**) by Salt Metathesis.** To a solution of {LON<sup>Ar</sup>}H<sub>2</sub> (0.45 g, 0.79 mmol) in toluene (10 mL) was added *n*-butyllithium (1.15 mL of a 1.37 M solution in hexane, 1.58 mmol) at 0 °C. The reaction mixture was stirred during 20 min at 0 °C and then during 30 min at room temperature. Volatiles were evaporated in vacuo, the solid residue was redissolved in THF (10 mL), and the obtained solution was added to a suspension of yttrium chloride (0.16 g, 0.79 mmol) in THF (10 mL) at room temperature. The reaction mixture was stirred during 12 h, after which time period a solution of Li[N(SiMe<sub>3</sub>)<sub>2</sub>](Et<sub>2</sub>O) (0.19 g, 0.79 mmol) in THF (10 mL) was added in at room temperature. The reaction mixture was stirred during 12 h,

volatiles were evaporated in vacuo, and the solid residue was extracted with toluene (20 mL). The clear solution was concentrated at 0 °C to afford **7** as colorless crystals (0.18 g, 0.13 mmol, 33%). Colorless crystals suitable for X-ray diffraction studies were obtained by slow concentration of a toluene solution at room temperature. <sup>1</sup>H NMR (pyridine-*d*<sub>5</sub>, 400 MHz, 25 °C):  $\delta$  7.94 (s, 1H,  $C_6H_3$ ), 7.44 (d, <sup>4</sup>J = 2.5, 1H,  $C_6H_2$ ), 7.27 (several mult, 11H,  $C_6H_3$ ,  $C_6H_2$ ), 7.03 (d, <sup>4</sup>J = 2.5, 1H,  $C_6H_2$ ), 6.67 (d, <sup>4</sup>J = 2.5, 1H,  $C_6H_2$ ), 6.38 (s, 1H,  $C_6H_3$ ), 3.70 (sept, <sup>3</sup>J = 6.8, 2H,  $CH(CH_3)_2$ ), 3.48 (sept, <sup>3</sup>J = 6.8, 2H,  $CH(CH_3)_2$ ), 3.41 (sept, <sup>3</sup>J = 6.8, <sup>3</sup>J = 6.8, 2H,  $CH(CH_3)_2$ ), 3.35 (sept, <sup>3</sup>J = 6.8, 2H,  $CH(CH_3)_2$ ), 1.59 (br s, 9H,  $C(CH_3)_3$ ), 1.58 (br s, 9H,  $C(CH_3)_3$ ), 1.30 (d, <sup>3</sup>J = 6.8, 6H,  $CH(CH_3)_2$ ), 1.26 (d, <sup>3</sup>J = 6.8, 6H,  $CH(CH_3)_2$ ), 1.21 (d, <sup>3</sup>J = 6.8, 6H,  $CH(CH_3)_2$ ), 1.12 (br s, 9H,  $C(CH_3)_3$  that overlapped with 6H,  $CH(CH_3)_2$ ), 0.99 (br s, 9H,  $C(CH_3)_3$  that overlapped with 6H,  $CH(CH_3)_2$ ), 0.96 (d, <sup>3</sup>J<sub>H,H</sub> = 6.8, 12H,  $CH(CH_3)_2$ ), 0.71 (d, <sup>3</sup>J = 6.8, 6H,  $CH(CH_3)_2$ ). <sup>7</sup>Li NMR (pyridine-*d*<sub>5</sub>, 156 MHz, 25 °C):  $\delta$  2.60. <sup>13</sup>C{<sup>1</sup>H} NMR (pyridine-*d*<sub>5</sub>, 100 MHz, 25 °C):  $\delta$  169.4 (CN<sub>2</sub>), 158.9 (O- $C_6H_2$ ), 157.6 (O- $C_6H_2$ ), 145.2 ( $C_6H_3$ -<sup>i</sup>Pr), 144.0 ( $C_6H_3$ -<sup>i</sup>Pr), 143.6 ( $C_6H_3$ -<sup>i</sup>Pr), 141.7 ( $C_6H_3$ -<sup>i</sup>Pr), 141.0 ( $C_6H_3$ -<sup>i</sup>Pr), 140.0 ( $C_6H_3$ -<sup>i</sup>Pr), 137.2 ( $C_6H_2$ -tBu), 136.1 ( $C_6H_2$ -tBu), 129.2 ( $C_6H_2$ ), 128.4 ( $C_6H_2$ ), 128.0 ( $C_6H_2$ ), 127.8 ( $C_6H_2$ ), 126.0 ( $N-C_6H_3$ ), 125.2 ( $N-C_6H_3$ ), 124.6 ( $C_6H_3$ ), 124.4 ( $C_6H_3$ ), 124.2 ( $C_6H_2$ ), 118.6 ( $C_6H_3$ ), 35.7 ( $Ph-C(CH_3)_3$ ), 35.4 ( $Ph-C(CH_3)_3$ ), 33.9 ( $Ph-C(CH_3)_3$ ), 33.6 ( $Ph-C(CH_3)_3$ ), 31.9 ( $Ph-C(CH_3)_3$ ), 31.2 ( $Ph-C(CH_3)_3$ ), 29.9 ( $Ph-C(CH_3)_3$ ), 29.6 ( $Ph-C(CH_3)_3$ ), 28.9 ( $Ph-CH(CH_3)_2$ ), 28.7 ( $Ph-CH(CH_3)_2$ ), 28.5 ( $Ph-CH(CH_3)_2$ ), 28.1 ( $Ph-CH(CH_3)_2$ ), 25.4 ( $Ph-CH(CH_3)_2$ ), 24.8 ( $Ph-CH(CH_3)_2$ ), 24.3 ( $Ph-CH(CH_3)_2$ ), 24.1 ( $Ph-CH(CH_3)_2$ ), 22.6 ( $Ph-CH(CH_3)_2$ ), 22.5 ( $Ph-CH(CH_3)_2$ ), 22.3 ( $Ph-CH(CH_3)_2$ ). IR (Nujol, KBr)  $\nu$  ( $cm^{-1}$ ): 1612 s, 1577 s, 1560 m, 1435 m, 1361 m, 1323 m, 1283 m, 1260 s, 1223 m, 1202 w, 1188 m, 1143 m, 1098 m, 1057 m, 1041 w, 964 m, 934 m, 886 m, 869 m, 833 m, 801 m, 786 m, 777 w, 768 w, 750 s, 694 m, 662 w, 642 m, 527 s. Anal. Calcd for  $C_{86}H_{124}LiN_4O_4Y$ : C, 75.19; H, 9.10; N, 4.08; Y, 6.47. Found: C, 75.48; H, 9.21; N, 4.15; Y, 6.13.

**[{(CyN)<sub>2</sub>CC<sub>6</sub>H<sub>2</sub>(tBu)<sub>2</sub>O<sub>2</sub>Y(N(SiMe<sub>3</sub>)<sub>2</sub>)<sub>2</sub>}{LON<sup>Cy</sup>}Y(N(SiMe<sub>3</sub>)<sub>2</sub>), 8].**  
 To a solution of Y[N(SiMe<sub>3</sub>)<sub>2</sub>]<sub>3</sub> (0.180 g, 0.313 mmol) in a toluene/THF mixture (1:10 v/v) (10 mL) was added a solution of {LON<sup>Cy</sup>}H<sub>2</sub> (0.129 g, 0.313 mmol) in toluene (10 mL). The reaction mixture was stirred at 50 °C during 120 h, and then volatiles were evaporated in vacuo. Hexamethyldisilazane was detected by chromatography, and its amount (0.64 mmol) was close to the theoretic one (0.62 mmol). The solid residue was recrystallized from DME to afford byproduct {LON<sup>Cy</sup>}<sub>2</sub>YLi(DME) (**10**) as colorless crystals (ca. 0.05 g). The supernatant solution was separated and concentrated in vacuo to afford **8** (0.180 g, 0.136 mmol, 87%) as a yellow crystalline powder. <sup>1</sup>H NMR ( $C_6D_6$ , 400 MHz, 25 °C):  $\delta$  7.58 (br s, 2H,  $C_6H_2$ ), 7.27 (br s, 2H,  $C_6H_2$ ), 3.60 (br m, 4H,  $CH(CH_3)_2$ ), 2.1–1.1 (several br m, 40H,  $CH(CH_3)_2$ ), 1.71 (s, 18H,  $C(CH_3)_3$ ), 1.34 (s, 18H,  $C(CH_3)_3$ ), 0.51 (br s, 36H, N(Si(CH<sub>3</sub>)<sub>3</sub>)<sub>2</sub>). <sup>13</sup>C{<sup>1</sup>H} NMR ( $C_6D_6$ , 100 MHz, 25 °C):  $\delta$  187.4 (CN<sub>2</sub>), 161.6 (O- $C_6H_2$ ), 137.3 ( $C_6H_2$ -tBu), 137.0 ( $C_6H_2$ -tBu), 125.3 ( $C_6H_2$ -CN<sub>2</sub>), 124.3 ( $C_6H_2$ ), 123.1 ( $C_6H_2$ ), 59.2 ( $CH(CH_3)_2$ ), 35.2 ( $C(CH_3)_3$ ), 34.7 ( $C(CH_3)_3$ ), 31.5 ( $C(CH_3)_3$ ), 29.5 ( $C(CH_3)_3$ ), 26.0–25.5 ( $CH(CH_3)_2$ ), 5.3 (N(Si(CH<sub>3</sub>)<sub>3</sub>)<sub>2</sub>). IR (Nujol, KBr)  $\nu$  ( $cm^{-1}$ ): 1617 s, 1594 m, 1362 m, 1303 s, 1258 s, 1238 w, 1219 m, 1201 m, 1145 m, 1124 m, 1090 w, 1067 m, 1027 w, 970 m, 889 s, 845 s, 824 w, 784 m, 677 m, 645 w, 617 w, 526 w. Anal. Calcd for  $C_{66}H_{120}N_6O_2Si_4Y_2$ : C, 60.06; H, 9.16; N, 6.37; Y, 13.47. Found: C, 60.20; H, 9.05; N, 6.25; Y, 13.2.

**{(CyN)<sub>2</sub>CC<sub>6</sub>H<sub>2</sub>(tBu)<sub>2</sub>O<sub>2</sub>YLi(DME)}<sub>2</sub>{LON<sup>Cy</sup>}<sub>2</sub>YLi(DME), 10.**  
 To a solution of {LON<sup>Cy</sup>}H<sub>2</sub> (0.982 g, 2.38 mmol) in toluene (10 mL) was added *n*-butyllithium (4.53 mL of a 1.05 M solution in hexane, 4.76 mmol) at 0 °C, and the reaction mixture was stirred during 20 min at 0 °C and then during 30 min at room temperature. Volatiles were evaporated in vacuo, the solid residue was redissolved in THF (10 mL), and the resulting solution was then added to a suspension of yttrium

chloride (0.233 g, 1.19 mmol) in THF (10 mL) at room temperature. The reaction mixture was stirred during 12 h, and then volatiles were evaporated in vacuo. The solid residue was extracted with toluene (30 mL), and toluene was evaporated in vacuo. The solid residue was redissolved in DME (20 mL), and the clear solution was concentrated at 0 °C to afford **10** as a white crystalline powder (0.539 g, 0.536 mmol, 45%). <sup>1</sup>H NMR (pyridine-*d*<sub>5</sub>, 400 MHz, 50 °C): δ 7.58 (br m, 2H, C<sub>6</sub>H<sub>2</sub>), 7.15 (br m, 2H, C<sub>6</sub>H<sub>2</sub>), 3.64 (br m, 4H, CH(CH<sub>2</sub>)<sub>5</sub>), 3.49 (br s, 6H, (CH<sub>3</sub>)<sub>2</sub> DME), 3.26 (br s, 4H, CH<sub>2</sub>, DME), 1.64 (br s, 18H, C(CH<sub>3</sub>)<sub>3</sub>), 2.0–1.0 (several m, 40H, CH(CH<sub>2</sub>)<sub>5</sub>), 1.40 (br s, 18H, C(CH<sub>3</sub>)<sub>3</sub>). <sup>7</sup>Li NMR (pyridine-*d*<sub>5</sub>, 155 MHz, 25 °C): δ 2.46. <sup>13</sup>C{<sup>1</sup>H} NMR (*d*<sub>5</sub>-py, 100 MHz, 25 °C): δ 162.6 (CN<sub>2</sub>), 162.2 (O-C<sub>6</sub>H<sub>2</sub>), 138.4 (C<sub>6</sub>H<sub>2</sub>-*t*Bu), 136.7 (C<sub>6</sub>H<sub>2</sub>-*t*Bu), 128.7 (C<sub>6</sub>H<sub>2</sub>-CN<sub>2</sub>), 126.2 (C<sub>6</sub>H<sub>2</sub>), 114.4 (C<sub>6</sub>H<sub>2</sub>), 72.1 (CH<sub>2</sub>, DME), 58.6 (CH<sub>3</sub>, DME), 35.6 (Ph-C(CH<sub>3</sub>)<sub>3</sub>), 34.8 (Ph-C(CH<sub>3</sub>)<sub>3</sub>), 31.8 (Ph-C(CH<sub>3</sub>)<sub>3</sub>), 30.0 (Ph-C(CH<sub>3</sub>)<sub>3</sub>), 27.1, 25.7, 25.3 (CH(CH<sub>2</sub>)<sub>5</sub>). IR (Nujol, KBr)  $\nu$  (cm<sup>-1</sup>): 1615 s, 1584 m, 1436 m, 1361 w, 1301 s, 1258 s, 1220 m, 1201 m, 1181 w, 1148 w, 1126 m, 1095 w, 1063 w, 1030 w, 939 s, 888 m, 840 s, 785 m, 753 m, 671 m, 525 m. Anal. Calcd for C<sub>58</sub>H<sub>94</sub>LiN<sub>4</sub>O<sub>4</sub>Y: C, 69.16; H, 9.41; N, 5.56; Y, 8.83. Found: C, 68.90; H, 9.52; N, 7.71; Y, 8.74.

{[(CyN)<sub>2</sub>CC<sub>6</sub>H<sub>2</sub>(*t*Bu)<sub>2</sub>O]NdN(SiMe<sub>3</sub>)<sub>2</sub>]<sub>2</sub> ({LON<sup>Cy</sup>}Nd(N-SiMe<sub>3</sub>)<sub>2</sub>, **9**). Using a protocol similar to that described above for **8**, compound **9** was obtained from Nd[N(SiMe<sub>3</sub>)<sub>2</sub>]<sub>3</sub> (0.43 g, 0.67 mmol) and {LON<sup>Cy</sup>}H<sub>2</sub> (0.28 g, 0.67 mmol). A similar workup afforded **9** as a cyan-blue crystalline powder (0.29 g, 40 mmol, 61%). Crystals suitable for X-ray diffraction studies were grown by slow concentration from a solution in a Et<sub>2</sub>O/hexane (1:10 v/v) mixture at room temperature. IR (Nujol, KBr)  $\nu$  (cm<sup>-1</sup>): 1619 s, 1411 w, 1362 m, 1300 s, 1258 s, 1201 w, 1180 m, 1149 w, 1125 w, 1094 w, 1063 m, 1028 w, 930 s, 884 m, 840 s, 753 w, 681 m, 618 w, 521 m. Anal. Calcd for C<sub>66</sub>H<sub>120</sub>N<sub>6</sub>O<sub>2</sub>Si<sub>4</sub>Nd<sub>2</sub>: C, 55.41; H, 8.46; N, 5.87; Nd, 20.17. Found: C, 55.70; H, 5.71; N, 6.01; Nd, 20.05.

**Reaction between Pro-ligand {LON<sup>Ar</sup>}H<sub>2</sub> and Y[N(SiMe<sub>3</sub>)<sub>2</sub>]<sub>3</sub>. Synthesis of {LO<sup>H</sup>N<sup>Ar</sup>}<sub>3</sub>Y (**11**). In the glovebox, a Teflon-valved NMR tube was charged with {LON<sup>Ar</sup>}H<sub>2</sub> (0.0225 g, 0.0393 mmol) and Y[N(SiMe<sub>3</sub>)<sub>2</sub>]<sub>3</sub> (0.0075 g, 0.0131 mmol). To this mixture, C<sub>6</sub>D<sub>6</sub> (0.6 mL) was vacuum-transferred in, and the tube was shaken for 24 h at room temperature. <sup>1</sup>H NMR indicated that **11** formed quantitatively. <sup>1</sup>H NMR (C<sub>6</sub>D<sub>6</sub>, 500 MHz, 25 °C): δ 7.45 (d, <sup>4</sup>J = 2.3, 3H, C<sub>6</sub>H<sub>2</sub>), 7.23 (d, <sup>3</sup>J = 7.6, 6H, C<sub>6</sub>H<sub>3</sub>), 7.15 (t, <sup>3</sup>J = 7.6, 3H, C<sub>6</sub>H<sub>3</sub>), 7.03 (t, <sup>3</sup>J = 7.6, 3H, C<sub>6</sub>H<sub>3</sub>), 6.93 (d, <sup>3</sup>J = 7.6, 6H, C<sub>6</sub>H<sub>3</sub>), 6.91 (d, <sup>4</sup>J = 2.3, 3H, C<sub>6</sub>H<sub>2</sub>), 6.02 (s, 3H, NH), 3.42 (hept, <sup>3</sup>J = 6.9, 6H, CH(CH<sub>3</sub>)), 3.16 (hept, <sup>3</sup>J = 6.9, 6H, CH(CH<sub>3</sub>)), 1.67 (s, 27H, C(CH<sub>3</sub>)), 1.29 (d, <sup>3</sup>J = 6.9, 18H, CH(CH<sub>3</sub>)), 1.23 (d, <sup>3</sup>J = 6.9, 18H, CH(CH<sub>3</sub>)), 0.98 (s, 27H, C(CH<sub>3</sub>)), 0.93 (d, <sup>3</sup>J = 6.7, 18H, CH(CH<sub>3</sub>)), 0.90 (d, <sup>3</sup>J = 6.9, 18H, CH(CH<sub>3</sub>)). <sup>13</sup>C{<sup>1</sup>H} NMR (C<sub>6</sub>D<sub>6</sub>, 100 MHz, 25 °C): δ 158.4 (CN<sub>2</sub>), 157.0 (O-C<sub>6</sub>H<sub>2</sub>), 144.4 (C<sub>6</sub>H<sub>3</sub>-*i*Pr), 140.4 (C<sub>6</sub>H<sub>3</sub>-*i*Pr), 137.5 (C<sub>6</sub>H<sub>2</sub>-*t*Bu), 137.1 (C<sub>6</sub>H<sub>2</sub>-*t*Bu), 135.1 (N-C<sub>6</sub>H<sub>3</sub>), 127.3 (C<sub>6</sub>H<sub>3</sub>), 126.0 (C<sub>6</sub>H<sub>2</sub>), 125.3 (C<sub>6</sub>H<sub>3</sub>), 124.1 (C<sub>6</sub>H<sub>3</sub>), 123.5 (C<sub>6</sub>H<sub>3</sub>), 113.3 (C<sub>6</sub>H<sub>2</sub>-CN<sub>2</sub>), 35.3 (Ph-C(CH<sub>3</sub>)<sub>3</sub>), 33.7 (Ph-C(CH<sub>3</sub>)<sub>3</sub>), 31.0 (Ph-C(CH<sub>3</sub>)<sub>3</sub>), 29.5 (Ph-C(CH<sub>3</sub>)<sub>3</sub>), 28.9 (Ph-CH(CH<sub>3</sub>)<sub>2</sub>), 28.7 (Ph-CH(CH<sub>3</sub>)<sub>2</sub>), 24.6 (Ph-CH(CH<sub>3</sub>)<sub>2</sub>), 24.4 (Ph-CH(CH<sub>3</sub>)<sub>2</sub>), 22.0 (Ph-CH(CH<sub>3</sub>)<sub>2</sub>), 21.9 (Ph-CH(CH<sub>3</sub>)<sub>2</sub>). IR (ATR module)  $\nu$  (cm<sup>-1</sup>): 3420 w, 2848 w, 1665 m, 1615 m, 1472 w, 1374 s, 1360 s, 1275 s, 1169 s, 1204 s, 1031 m, 931 w, 885 m, 701 m, 682 m, 623 w. Anal. Calcd for C<sub>117</sub>H<sub>165</sub>N<sub>6</sub>O<sub>3</sub>Y: C, 78.40; H, 9.28; N, 4.69. Found: C, 78.89; H, 10.01; N, 4.80.**

{[(*i*PrN)<sub>2</sub>CC<sub>6</sub>H<sub>2</sub>(*t*Bu)<sub>2</sub>O]YMe<sub>2</sub>Li(TMEDA)]<sub>2</sub>Et<sub>2</sub>O ({LON<sup>*i*Pr</sup>}<sub>2</sub>YMe<sub>2</sub>Li<sub>2</sub>(TMEDA)<sub>2</sub>, **12**). To a suspension of yttrium chloride (0.140 g, 0.70 mmol) and TMEDA (0.42 mL, 2.80 mmol) in THF (10 mL) was added methyllithium (3.29 mL of a 0.85 M solution in Et<sub>2</sub>O, 2.80 mmol) at -20 °C, and the reaction mixture was stirred for 10 min at 0 °C. During this time period, all the solids dissolved. To the resulting solution was added a solution of {LON<sup>*i*Pr</sup>}H<sub>2</sub> (0.23 g, 0.70 mmol) in THF (10 mL), and the reaction mixture was stirred for 30 min at 0 °C. Volatiles were evaporated in vacuo, and the residue was

extracted with diethyl ether (20 mL). The clear solution was concentrated at 0 °C to afford **12** as a white crystalline powder (0.25 g, 0.205 mmol, 59%). Colorless crystals suitable for X-ray diffraction studies were grown by slow concentration from a diethyl ether solution. <sup>1</sup>H NMR (C<sub>6</sub>D<sub>6</sub>, 200 MHz, 25 °C): δ 7.65 (d, <sup>4</sup>J = 2.5, 2H, C<sub>6</sub>H<sub>2</sub>), 7.39 (d, <sup>4</sup>J = 2.5, 2H, C<sub>6</sub>H<sub>2</sub>), 4.6 (sept, <sup>3</sup>J = 6.4, 4H, CH(CH<sub>3</sub>)<sub>2</sub>), 3.28 (q, <sup>3</sup>J = 7.0, 4H, CH<sub>2</sub>, Et<sub>2</sub>O), 2.02 (br s, 24H, CH<sub>3</sub>, TMEDA), 1.92 (s, 18H, C(CH<sub>3</sub>)<sub>3</sub>), 1.73 (br m, 4H, CH<sub>2</sub>, TMEDA), 1.46 (br s, 18H, C(CH<sub>3</sub>)<sub>3</sub>) that overlapped with 24H, CH(CH<sub>3</sub>)<sub>2</sub>), 1.12 (t, <sup>3</sup>J = 7.0, 6H, CH<sub>3</sub>, Et<sub>2</sub>O), -0.38 (br s, 12H, YCH<sub>3</sub>). <sup>7</sup>Li NMR (C<sub>6</sub>D<sub>6</sub>, 78 MHz, 20 °C): δ 3.58. <sup>13</sup>C NMR (C<sub>6</sub>D<sub>6</sub>, 50 MHz, 25 °C): δ 185.2 (CN<sub>2</sub>), 163.2 (O-C<sub>6</sub>H<sub>2</sub>), 136.3 (C<sub>6</sub>H<sub>2</sub>-*t*Bu), 134.6 (C<sub>6</sub>H<sub>2</sub>-*t*Bu), 126.1 (C<sub>6</sub>H<sub>2</sub>-CN<sub>2</sub>), 123.7 (C<sub>6</sub>H<sub>2</sub>), 122.3 (C<sub>6</sub>H<sub>2</sub>), 65.6 (CH<sub>2</sub>, Et<sub>2</sub>O), 56.8 (CH<sub>2</sub>, TMEDA), 49.4 (CH(CH<sub>3</sub>)<sub>2</sub>), 45.9 (CH<sub>3</sub>, TMEDA), 35.5 (C(CH<sub>3</sub>)<sub>3</sub>), 34.0 (C(CH<sub>3</sub>)<sub>3</sub>), 32.0 (CH(CH<sub>3</sub>)<sub>2</sub>), 30.2 (C(CH<sub>3</sub>)<sub>3</sub>), 25.7 (C(CH<sub>3</sub>)<sub>3</sub>), 15.3 (CH<sub>3</sub>, Et<sub>2</sub>O), 11.2 (Y(CH<sub>3</sub>)<sub>2</sub>). IR (Nujol, KBr)  $\nu$  (cm<sup>-1</sup>): 1601 m, 1554 s, 1492 s, 1413 m, 1360 m, 1302 s, 1270 w, 1256 w, 1229 w, 1201 w, 1181 m, 1159 w, 1151 w, 1124 s, 1067 s, 1035 s, 1018 s, 949 s, 897 w, 882 m, 860 w, 843 s, 791 s, 774 w, 758 s, 705 w, 643 w, 588 m, 580 m, 525 m, 499 m. Anal. Calcd for C<sub>62</sub>H<sub>122</sub>Li<sub>2</sub>N<sub>8</sub>O<sub>3</sub>Y<sub>2</sub>: C, 61.07; H, 10.08; N, 9.19; Y, 14.58. Found: C, 61.38; H, 9.95; N, 9.11; Y, 14.28.

{[(CyN)<sub>2</sub>CC<sub>6</sub>H<sub>2</sub>(*t*Bu)<sub>2</sub>O]YMe<sub>2</sub>Li(TMEDA)]<sub>2</sub>Et<sub>2</sub>O ({LON<sup>Cy</sup>}<sub>2</sub>YMe<sub>2</sub>Li<sub>2</sub>(TMEDA)<sub>2</sub>, **13**). Using a protocol similar to that described above for **12**, complex **13** was obtained from YCl<sub>3</sub> (0.072 g, 0.368 mmol), TMEDA (0.22 mL, 1.47 mmol), methyllithium (1.73 mL of a 0.85 M solution in Et<sub>2</sub>O, 1.47 mmol), and {LON<sup>Cy</sup>}H<sub>2</sub> (0.152 g, 0.368 mmol). A similar workup afforded **13** as a pale yellow crystalline powder (0.173 g, 0.125 mmol, 68%). Crystals suitable for X-ray diffraction studies were grown by slow concentration of a Et<sub>2</sub>O solution at room temperature. <sup>1</sup>H NMR (C<sub>6</sub>D<sub>6</sub>, 200 MHz, 25 °C): δ 7.61 (d, <sup>4</sup>J = 2.5, 2H, C<sub>6</sub>H<sub>2</sub>), 7.41 (d, <sup>4</sup>J = 2.5, 2H, C<sub>6</sub>H<sub>2</sub>), 3.59 (br m, 4H, CH(CH<sub>2</sub>)<sub>5</sub>), 3.25 (q, <sup>3</sup>J = 7.0, 4H, CH<sub>2</sub>, Et<sub>2</sub>O), 2.04 (br s, 24H, CH<sub>3</sub>, TMEDA), 1.93 (br s, 18H, C(CH<sub>3</sub>)<sub>3</sub>), 1.9–1.0 (several m, 4H, CH<sub>2</sub>, TMEDA that overlapped with 40H, CH(CH<sub>2</sub>)<sub>5</sub>), 1.44 (br s, 18H, C(CH<sub>3</sub>)<sub>3</sub>), 1.12 (tr, <sup>3</sup>J = 7.0, 6H, CH<sub>3</sub>, Et<sub>2</sub>O), -0.39 (br s, 12H, YCH<sub>3</sub>). <sup>7</sup>Li NMR (C<sub>6</sub>D<sub>6</sub>, 78 MHz, 25 °C): δ 3.64. <sup>13</sup>C{<sup>1</sup>H} NMR (C<sub>6</sub>D<sub>6</sub>, 50 MHz, 25 °C): δ 185.5 (CN<sub>2</sub>), 163.3 (O-C<sub>6</sub>H<sub>2</sub>), 135.8 (C<sub>6</sub>H<sub>2</sub>-*t*Bu), 134.4 (C<sub>6</sub>H<sub>2</sub>-*t*Bu), 126.2 (C<sub>6</sub>H<sub>2</sub>-CN<sub>2</sub>), 123.5 (C<sub>6</sub>H<sub>2</sub>), 122.8 (C<sub>6</sub>H<sub>2</sub>), 65.6 (CH<sub>2</sub>, Et<sub>2</sub>O), 59.0 (CH(CH<sub>2</sub>)<sub>2</sub>), 56.7 (CH<sub>2</sub>, TMEDA), 45.9 (CH<sub>3</sub>, TMEDA), 35.4 (Ph-C(CH<sub>3</sub>)<sub>3</sub>), 34.0 (Ph-C(CH<sub>3</sub>)<sub>3</sub>), 32.0 (Ph-C(CH<sub>3</sub>)<sub>3</sub>), 30.2 (Ph-C(CH<sub>3</sub>)<sub>3</sub>), 27.0, 26.6, 26.4 (CH(CH<sub>2</sub>)<sub>5</sub>), 15.3 (CH<sub>3</sub>, Et<sub>2</sub>O), 10.5 (Y(CH<sub>3</sub>)<sub>2</sub>). IR (Nujol, KBr)  $\nu$  (cm<sup>-1</sup>): 1606 m, 1523 m, 1437 m, 1360 w, 1303 s, 1265 m, 1218 w, 1200 w, 1180 w, 1150 m, 1129 m, 1097 w, 1066 w, 1033 m, 989 w, 949 m, 885 m, 842 s, 791 m, 741 w, 660 w, 549 w, 528 m. Anal. Calcd for C<sub>74</sub>H<sub>138</sub>Li<sub>2</sub>N<sub>8</sub>O<sub>3</sub>Y<sub>2</sub>: C, 64.42; H, 10.08; N, 8.12; Y, 12.89. Found: C, 64.07; H, 9.80; N, 8.07; Y, 12.95.

{[(*i*PrN)<sub>2</sub>CC<sub>6</sub>H<sub>2</sub>(*t*Bu)<sub>2</sub>O]NdMe<sub>2</sub>Li(TMEDA)]<sub>2</sub> ({LON<sup>*i*Pr</sup>}<sub>2</sub>NdMe<sub>2</sub>Li<sub>2</sub>(TMEDA)<sub>2</sub>, **14**). Using a protocol similar to that described above for **12**, complex **14** was obtained from NdCl<sub>3</sub> (0.143 g, 0.57 mmol), TMEDA (0.34 mL, 2.28 mmol), methyllithium (2.68 mL of a 0.85 M solution in Et<sub>2</sub>O, 2.28 mmol), and {LON<sup>*i*Pr</sup>}H<sub>2</sub> (0.190 g, 0.57 mmol). A similar workup afforded **14** as a cyan-blue crystalline powder (0.265 g, 0.196 mmol, 69%). Crystals suitable for X-ray diffraction studies were grown by slow concentration from a toluene solution at -20 °C. IR (Nujol, KBr)  $\nu$  (cm<sup>-1</sup>): 1602 m, 1562 w, 1413 w, 1358 w, 1329 m, 1294 s, 1258 w, 1229 w, 1200 w, 1178 s, 1157 w, 1125 s, 1065 w, 1034 m, 1018 m, 948 m, 882 m, 839 s, 790 m, 761 m, 690 w, 582 m, 524 m. Anal. Calcd for C<sub>65</sub>H<sub>120</sub>Li<sub>2</sub>N<sub>8</sub>O<sub>2</sub>Nd<sub>2</sub>: C, 57.91; H, 8.97; N, 8.31; Nd, 21.40. Found: C, 58.12; H, 9.01; N, 8.55; Nd, 21.80.

{[(*i*PrN)<sub>2</sub>CC<sub>6</sub>H<sub>2</sub>(*t*Bu)<sub>2</sub>O]SmMe<sub>2</sub>Li(TMEDA)]<sub>2</sub> · {LON<sup>*i*Pr</sup>}<sub>2</sub>Sm<sub>2</sub>Me<sub>2</sub>(OH)<sub>2</sub>Li<sub>2</sub>(TMEDA)<sub>2</sub>, **15**). Using a protocol similar to that described above for **12**, complex **15** was obtained from SmCl<sub>3</sub> (0.154 g, 0.60 mmol), TMEDA (0.36 mL, 2.40 mmol), methyllithium (2.84 mL of a 0.85 M solution in Et<sub>2</sub>O, 2.40 mmol), and {LON<sup>*i*Pr</sup>}H<sub>2</sub> (0.195 g,

0.60 mmol). A similar workup afforded **15** as a yellow crystalline powder (0.261 g, 0.192 mmol, 64%). Crystals suitable for X-ray diffraction studies were obtained by slow concentration of a toluene solution at  $-20\text{ }^{\circ}\text{C}$ . IR (Nujol, KBr)  $\nu$  ( $\text{cm}^{-1}$ ): 1605 m, 1495 w, 1410 w, 1358 m, 1329 m, 1292 s, 1267 m, 1256 w, 1229 w, 1200 m, 1175 m, 1157 w, 1124 m, 1065 w, 1032 s, 1018 m, 948 m, 839 s, 789 m, 760 m, 694 w. Anal. Calcd for  $\text{C}_{65}\text{H}_{120}\text{Li}_2\text{N}_8\text{O}_2\text{Sm}_2$ : C, 57.39; H, 8.89; N, 8.24; Sm, 22.11. Found: C, 57.25; H, 8.75; N, 8.29; Sm, 21.8.

$[\{\{\text{Pr}^{\text{N}}\}_2\text{CC}_6\text{H}_2(\text{tBu})_2\text{O}\}\text{Yb}(\text{OH})\text{MeLi}(\text{TMEDA})_2\text{Et}_2\text{O} (\{\{\text{LON}^{\text{Pr}}\}_2\text{Yb}_2\text{Me}_2(\text{OH})_2\text{Li}_2(\text{TMEDA})_2, \text{16})$ . Using a protocol similar to that described above for **12**, compound **16** was obtained from  $\text{YbCl}_3$  (0.129 g, 0.46 mmol), TMEDA (0.27 mL, 1.84 mmol), methyllithium (2.16 mL of a 0.85 M solution in  $\text{Et}_2\text{O}$ , 1.84 mmol), and  $\{\text{LON}^{\text{Pr}}\}_2\text{H}_2$  (0.153 g, 0.46 mmol). A similar workup afforded **16** as a yellow crystalline powder (0.210 g, 0.165 mmol, 65%). Crystals suitable for X-ray diffraction studies were grown by slow concentration of a  $\text{Et}_2\text{O}$  solution at room temperature. IR (Nujol, KBr)  $\nu$  ( $\text{cm}^{-1}$ ): 1601 m, 1528 m, 1411 w, 1298 s, 1266 w, 1248 m, 1222 w, 1194 w, 1172 w, 1149 m, 1130 w, 1113 m, 1068 m, 1037 m, 1022 m, 948 s, 886 s, 844 s, 790 m, 756 m, 740 m, 644 w, 602 m, 584 w. Anal. Calcd for  $\text{C}_{60}\text{H}_{118}\text{Li}_2\text{N}_8\text{O}_3\text{Yb}_2$ : C, 51.79; H, 8.55; N, 8.05; Yb, 24.87. Found: C, 51.85; H, 8.65; N, 8.22; Yb, 24.83.

**Crystal Structure Determination of  $[\{\{\text{LON}^{\text{Pr}}\}_2\text{Li}_2(\text{THF})_2\} \cdot (\text{THF}) (1), \{\{\text{LON}^{\text{Ar}}\}_2\text{Li}_2(\text{THF})_3 (2), \{\text{LO}^{\text{H}^{\text{N}^{\text{Ar}}}\}\text{YCl}_2(\text{DME}) (5), \{\text{LON}^{\text{Pr}}\}_2\text{Yn}(\text{SiMe}_3)_2 (6), \{\text{LON}^{\text{Ar}}\}_2\text{YLi}(\text{THF})_2 (7), \{\text{LON}^{\text{Cy}}\}_2\text{Nd}(\text{N}(\text{SiMe}_3)_2) (9), \{\text{LON}^{\text{Cy}}\}_2\text{YLi}(\text{DME}) (10), \{\text{LON}^{\text{Pr}}\}_2\text{Y}_2\text{Me}_4\text{Li}_2(\text{TMEDA})_2(\text{Et}_2\text{O}) (12), \{\text{LON}^{\text{Cy}}\}_2\text{Y}_2\text{Me}_4\text{Li}_2(\text{TMEDA})_2 \cdot (\text{Et}_2\text{O}) (13), \text{and } \{\text{LON}^{\text{Pr}}\}_2\text{Yb}_2\text{Me}_2(\text{OH})_2\text{Li}_2(\text{TMEDA})_2 \cdot (\text{Et}_2\text{O}) (16)$ .** Diffraction data were collected at 100(2) or 150(2) K using a Bruker APEX CCD diffractometer with graphite-monochromatized  $\text{MoK}\alpha$  radiation ( $\lambda = 0.71073\text{ \AA}$ ). A combination of  $\omega$  and  $\phi$  scans was carried out to obtain a unique data set. The crystal structures were solved by direct methods, and remaining atoms were located from difference Fourier synthesis, followed by full-matrix least-squares refinement based on  $F^2$  (programs SIR97 and SHELXL-97).<sup>34</sup> Many hydrogen atoms could be located from the Fourier difference analysis. Other hydrogen atoms were placed at calculated positions and forced to ride on the attached atom. The hydrogen atom positions were calculated, but not refined. All non-hydrogen atoms were refined with anisotropic displacement parameters. Crystal data and details of data collection and structure refinement for the different compounds are given in Tables S1 and S2 in the Supporting Information. Detailed crystallographic data (excluding structure factors) are available in the Supporting Information, as CIF files.

**Typical Procedure for Polymerization of *rac*-Lactide.** In a typical experiment (Table 3, entry 2), in the glovebox, a Schlenk flask was charged with a solution of **6** (10.0 mg, 17.2  $\mu\text{mol}$ ) in toluene (0.5 mL). *rac*-Lactide (0.248 g, 1.72 mmol, 100 equiv vs **Y**) in toluene (1.2 mL) was added rapidly to this solution. The mixture was immediately stirred with a magnetic stir bar at  $20\text{ }^{\circ}\text{C}$  for 1.33 h. The reaction was quenched by adding ca. 1.0 mL of a 10%  $\text{H}_2\text{O}$  solution in THF, and the polymer was precipitated from  $\text{CH}_2\text{Cl}_2$ /pentane (ca. 2:100 mL) five times. The polymer was then filtered and dried in vacuo to a constant weight.

## ASSOCIATED CONTENT

**Supporting Information.** Crystallographic data and details of data collection and structure refinement for  $[\{\{\text{LON}^{\text{Pr}}\}_2\text{Li}_2(\text{THF})_2\} \cdot (\text{THF}) (1), \{\{\text{LON}^{\text{Ar}}\}_2\text{Li}_2(\text{THF})_3 (2), \{\text{LO}^{\text{H}^{\text{N}^{\text{Ar}}}\}\text{YCl}_2(\text{DME}) (5), \{\text{LON}^{\text{Pr}}\}_2\text{Yn}(\text{SiMe}_3)_2 (6), \{\text{LON}^{\text{Ar}}\}_2\text{YLi}(\text{THF})_2 (7), \{\text{LON}^{\text{Cy}}\}_2\text{Nd}(\text{N}(\text{SiMe}_3)_2) (9), \{\text{LON}^{\text{Cy}}\}_2\text{YLi}(\text{DME}) (10), \{\text{LON}^{\text{Pr}}\}_2\text{Y}_2\text{Me}_4\text{Li}_2(\text{TMEDA})_2(\text{Et}_2\text{O}) (12), \{\text{LON}^{\text{Cy}}\}_2\text{Y}_2\text{Me}_4\text{Li}_2(\text{TMEDA})_2 \cdot (\text{Et}_2\text{O}) (13), \text{and } \{\text{LON}^{\text{Pr}}\}_2\text{Yb}_2\text{Me}_2(\text{OH})_2\text{Li}_2(\text{TMEDA})_2 \cdot (\text{Et}_2\text{O}) (16)$  as Tables S1 and S2 and CIF files, and representative  $^1\text{H}$  and  $^{13}\text{C}$  NMR spectra for some complexes. This material is available free of charge via the Internet at <http://pubs.acs.org>.

## AUTHOR INFORMATION

### Corresponding Author

\*E-mail: [evgueni.kirillov@univ-rennes1.fr](mailto:evgueni.kirillov@univ-rennes1.fr) (E.K.), [trif@iomc.ras.ru](mailto:trif@iomc.ras.ru) (A.T.), [jean-francois.carpentier@univ-rennes1.fr](mailto:jean-francois.carpentier@univ-rennes1.fr) (J.-F.C.).

## ACKNOWLEDGMENT

This work was supported by the GDRI “CH2D” between RAS Chemistry and Material Science Division and CNRS, the Russian Foundation for Basic Research (Grant 11-03-00555-a), the CNRS, and the Institut Universitaire de France (IUF).

## REFERENCES

- (1) For leading reviews on the synthesis of metal phenoxides, see: (a) Bochkarev, M. N.; Zakharov, L. N.; Kalinina, G. S. *Organoderivatives of Rare Earth Elements*; Nauka: Moscow, 1989. (b) Bradley, D. C.; Mehrotra, R. C.; Rothwell, I. P.; Singh, A. *Alkoxo and Aryloxo Derivatives of Metals*; Academic Press: New York, 2001.
- (2) For selected recent reviews on the synthesis of metal amidinates, see: (a) Trifonov, A. A. *Coord. Chem. Rev.* **2010**, *254*, 1327–1347. (b) Edelmann, F. T. *Chem. Soc. Rev.* **2009**, *38*, 2253–2268.
- (3) (a) Dubois, P.; Coulembier, O.; Raquez, J.-M., Eds. *Handbook of Ring-Opening Polymerization*; Wiley-VCH Verlag GmbH & Co. KGaA: Weinheim, Germany, 2009. (b) Dechy-Cabaret, O.; Martin-Vaca, B.; Bourissou, D. *Chem. Rev.* **2004**, *104*, 6147–6176. (c) Stanford, M. J.; Dove, A. P. *Chem. Soc. Rev.* **2010**, *39*, 486–494. (d) Thomas, C. M. *Chem. Soc. Rev.* **2010**, *39*, 165–173.
- (4) For selected leading references on the use of rare-earth phenoxide complexes in ROP catalysis, see: (a) Ovitt, T. M.; Coates, G. W. *J. Am. Chem. Soc.* **2002**, *124*, 1316–1326. (b) Ma, H.; Spaniol, T. P.; Okuda, J. *Dalton Trans.* **2003**, 4770–4780. (c) Ma, H.; Okuda, J. *Macromolecules* **2005**, *38*, 2665–2673. (d) Ma, H.; Spaniol, T. P.; Okuda, J. *Angew. Chem., Int. Ed.* **2006**, *45*, 7818–7821. (e) Buffet, J.-C.; Okuda, J. *Chem. Commun.* **2011**, *47*, 4796–4798. (f) Cai, C.-X.; Amgoune, A.; Lehmann, C. W.; Carpentier, J.-F. *Chem. Commun.* **2004**, 330–331. (g) Amgoune, A.; Thomas, C. M.; Roisnel, T.; Carpentier, J.-F. *Chem.—Eur. J.* **2006**, *12*, 169–179. (f) Castro, P. M.; Zhao, G.; Amgoune, A.; Thomas, C. M.; Carpentier, J.-F. *Chem. Commun.* **2006**, 4509–4511. (i) Amgoune, A.; Thomas, C. M.; Ilinca, S.; Roisnel, T.; Carpentier, J.-F. *Angew. Chem., Int. Ed.* **2006**, *45*, 2782–2784. (j) Liu, X.; Chang, X.; Tang, T.; Hu, N.; Pei, F.; Cui, D.; Chen, X.; Jing, X. *Organometallics* **2007**, *26*, 2747–2757. (k) Kramer, J. W.; Treiter, D. S.; Dunn, E. W.; Castro, P. M.; Roisnel, T.; Thomas, C. M.; Coates, G. W. *J. Am. Chem. Soc.* **2009**, *131*, 16042. (l) Bouyahy, M.; Ajellal, N.; Kirillov, E.; Thomas, C. M.; Carpentier, J.-F. *Chem.—Eur. J.* **2011**, *17*, 1872–1883. (m) Grunova, E.; Kirillov, E.; Roisnel, T.; Carpentier, J.-F. *Dalton Trans.* **2010**, *39*, 6739–6752. (n) Bonnet, F.; Cowley, A. R.; Mountford, P. *Inorg. Chem.* **2005**, *44*, 9046–9055. (o) Dyer, H. E.; Huijster, S.; Schwarz, A. D.; Wang, C.; Duchateau, R.; Mountford, P. *Dalton Trans.* **2008**, 32–35.
- (5) For selected leading references on the use of rare-earth amidinate complexes in ROP catalysis, see: (a) Reference 2b. (b) Giesbrecht, G. R.; Whitener, G. D.; Arnold, J. *Dalton Trans.* **2001**, 923–927. (c) Kui, S. C. F.; Li, H.-W.; Lee, H. K. *Inorg. Chem.* **2003**, *42*, 2824–2826. (d) Xu, X.; Zhang, Z.; Yao, Y.; Zhang, Y.; Shen, Q. *Inorg. Chem.* **2007**, *46*, 9379–9388. (e) Ajellal, N.; Lyubov, D. M.; Sinenkov, M. A.; Fukin, G. K.; Cherkasov, A. V.; Thomas, C. M.; Carpentier, J.-F.; Trifonov, A. A. *Chem.—Eur. J.* **2008**, *14*, 5440–5448. (f) Mahrova, T. V.; Fukin, G. K.; Cherkasov, A. V.; Trifonov, A. A. *Inorg. Chem.* **2009**, *48*, 4258–4266.
- (6) (a) Aubrecht, K. B.; Chang, K.; Hillmyer, M. A.; Tolman, W. B. *J. Polym. Sci., Polym. Chem. Ed.* **2001**, *39*, 284–293. (b) Wang, J.; Yao, Y.; Shen, Q. *Inorg. Chem.* **2009**, *48*, 744–751. (c) Qin, D.; Han, F.; Yao, Y.; Zhang, Y.; Shen, Q. *Dalton Trans.* **2009**, 5535–5541.
- (7) For the initial design of this ligand system, see: (a) Shapiro, P. J.; Bunel, E.; Schaefer, W. P.; Bercaw, J. E. *Organometallics* **1990**, *9*, 867–869.

(b) Shapiro, P. J.; Cotter, W. D.; Schaefer, W. P.; Labinger, J. A.; Bercaw, J. E. *J. Am. Chem. Soc.* **1994**, *116*, 4623–4640.

(8) These distances are in the usual range of Li–O bond lengths (1.818(3)–1.990(4) Å) found in dimeric lithium phenoxides [Li(OAr)(Solv)]<sub>2</sub> (where Ar = substituted phenyl group, Solv = Et<sub>2</sub>O, THF, or pyridine). See: (a) Cetinkaya, B.; Gumrukcu, I.; Lappert, M. F.; Atwood, J. L.; Shakir, R. *J. Am. Chem. Soc.* **1980**, *102*, 2086–2088. (b) Clegg, W.; Lamb, E.; Liddle, S. T.; Snaith, R.; Wheatley, R. E. H. *J. Organomet. Chem.* **1999**, *573*, 305–312. (c) Boyle, T. J.; Pedrotty, D. M.; Alam, T. M.; Vick, S. C.; Rodriguez, M. A. *Inorg. Chem.* **2000**, *39*, 5133–5146.

(9) These distances are on the long side of the usual range of Li–N bond lengths (1.995(9)–2.018(5) Å) found in the amidinate complexes of lithium. See: (a) Schmidt, J. A. R.; Arnold, J. J. *Chem. Soc., Dalton Trans.* **2002**, 2890–2899. (b) Baker, R. J.; Jones, C. *Organomet. Chem.* **2006**, *691*, 65–71.

(10) (a) Emslie, D. J. H.; Piers, W. E.; Parvez, M.; McDonald, R. *Organometallics* **2002**, *21*, 4226–4240. (b) Williams, S. E.; Sinenkov, M. A.; Fukin, G. K.; Sheridan, K.; Lynam, J. M.; Trifonov, A. A.; Kerton, F. M. *Dalton Trans.* **2008**, 3592–3598. (c) Miao, W.; Li, S.; Zhang, H.; Cui, D.; Wang, Y.; Huang, B. *J. Organomet. Chem.* **2007**, *692*, 4828–4834.

(11) (a) Duchateau, R.; van Wee, C.; Meetsma, A.; van Duijnen, P. T.; Teuben, J. H. *Organometallics* **1996**, *15*, 2279–2290. (b) Bambirra, S.; Brandsma, M. J. R.; Brussee, E. A. C.; Mettsma, A.; Hessen, B.; Teuben, J. H. *Organometallics* **2000**, *19*, 3179–3204. (c) Bambirra, S.; Meetsma, A.; Hessen, B.; Teuben, J. H. *Organometallics* **2001**, *20*, 782–785. (d) Lu, Z.; Yap, G. P. A.; Richeson, D. S. *Organometallics* **2001**, *20*, 706–712. (e) Trifonov, A. A.; Skvortsov, G. G.; Lyubov, D. M.; Skorodumova, N. A.; Fukin, G. K.; Baranov, E. V.; Glushakova, V. N. *Chem.—Eur. J.* **2006**, *12*, 5320–5327. (f) Trifonov, A. A.; Lyubov, D. M.; Fedorova, E. A.; Fukin, G. K.; Schumann, H.; Mühle, S.; Hummert, M.; Bochkarev, M. N. *Eur. J. Inorg. Chem.* **2006**, 747–756. (g) Trifonov, A. A.; Lyubov, D. M.; Fukin, G. K.; Baranov, E. V.; Kurskii, Yu. A. *Organometallics* **2006**, *25*, 3935–3942.

(12) (a) Long, D. P.; Chandrasekaran, A.; Day, R. O.; Bianconi, P. A.; Rheingold, A. L. *Inorg. Chem.* **2000**, *39*, 4476–4487. (b) Gao, W.; Cui, D. *J. Am. Chem. Soc.* **2008**, *130*, 4984–4991. (c) Wei, X.; Cheng, Y.; Hitchcock, P. B.; Lappert, M. F. *Dalton Trans.* **2008**, 5235–5246. (d) Lyubov, D. M.; Fukin, G. K.; Trifonov, A. A. *Inorg. Chem.* **2007**, *46*, 11450–11456.

(13) Otero, A.; Fernández-Baeza, J.; Antiñolo, A.; Tejada, J.; Lara-Sánchez, A.; Sánchez-Barba, L. F.; López-Solera, I.; Rodriguez, A. M. *Inorg. Chem.* **2007**, *46*, 1760–1770.

(14) Xia, A.; El-Kalderi, H. M.; Heeg, M. J.; Winter, C. H. *J. Organomet. Chem.* **2003**, *682*, 224–232.

(15) (a) Zhou, S.; Wang, W.; Yang, G.; Li, Q.; Zhang, L.; Yao, Z.; Zhou, Z.; Song, H. *Organometallics* **2007**, *26*, 3755–3761. (b) Lee, M. H.; Hwang, J.-W.; Kim, Y.; Kim, J.; Han, Y.; Do, Y. *Organometallics* **1999**, *18*, 5124–5129. (c) Hodgson, L. M.; Platel, R. H.; White, A. J. P.; Williams, C. K. *Macromolecules* **2008**, *41*, 8603–8607.

(16) For covalent Y–N bond lengths in five-coordinate complexes, see: (a) Graf, D. D.; Davis, W. M.; Schrock, R. R. *Organometallics* **1998**, *17*, 5820–5824. (b) Avent, A. G.; Cloke, F. G. N.; Elvidge, B. R.; Hitchcock, P. B. *Dalton Trans.* **2004**, 1083–1096. (c) Lyubov, D. M.; Döring, C.; Fukin, G. K.; Cherkasov, A. V.; Shavyrin, A. S.; Kempe, R.; Trifonov, A. A. *Organometallics* **2008**, *27*, 2905–2907. (d) Hultsch, K. C.; Hampel, F.; Wagner, T. *Organometallics* **2004**, *23*, 2601–2612.

(17) (a) Chen, H.; Barlett, R. A.; Rasika Dias, H. V.; Olmstead, M. M.; Power, P. P. *Inorg. Chem.* **1991**, *30*, 2487–2494. (b) Andrews, P. C.; Deacon, G. B.; Forsyth, C. M.; Scott, N. M. *Angew. Chem., Int. Ed.* **2001**, *40*, 2108–2111. (c) Carey, D. T.; Mair, F. S.; Pritchard, R. G.; Warren, J. E.; Woods, J. E. *Eur. J. Inorg. Chem.* **2003**, 3464–3471. (d) Cole, M. L.; Davies, A. J.; Jones, C.; Junk, P. C. *J. Organomet. Chem.* **2004**, *689*, 3093–3107. (e) Jin, G.; Jones, C.; Junk, P.; Lippert, K.-A.; Rose, R.; Stasch, A. *New J. Chem.* **2009**, *33*, 64–75.

(18) (a) Ruhlandt-Senge, K.; Ellison, J. J.; Wehmschulte, R. J.; Pauer, F.; Power, P. P. *J. Am. Chem. Soc.* **1993**, *115*, 11353–11357. (b) Schiemenz, B.; Power, P. P. *Angew. Chem., Int. Ed.* **1996**, *35*, 2150–2152. (c) Wehmschulte,

R. J.; Power, P. P. *J. Am. Chem. Soc.* **1997**, *119*, 2847–2852. (d) Dinnebier, R. E.; Behrens, U.; Olbrich, F. *J. Am. Chem. Soc.* **1998**, *120*, 1430–1433.

(19) Deacon, G. B.; Feng, T.; Junk, P. C.; Skelton, B. W.; White, A. H. *Z. Anorg. Allg. Chem.* **2006**, *632*, 1986–1988.

(20) (a) Villiers, C.; Thuéry, P.; Ephritikhine, M. *Eur. J. Inorg. Chem.* **2004**, 4624–4632. (b) Luo, Y.; Yao, Y.; Shen, Q.; Yu, K.; Weng, L. *Eur. J. Inorg. Chem.* **2003**, 318–323. (c) Yao, Y.; Luo, Y.; Chen, J.; Zhang, Z.; Zhang, Y.; Shen, Q. *J. Organomet. Chem.* **2003**, 229–237. (d) Skvortsov, G. G.; Yakovenko, M. V.; Castro, P. M.; Fukin, G. K.; Cherkasov, A. V.; Carpentier, J.-F.; Trifonov, A. A. *Eur. J. Inorg. Chem.* **2007**, 3260–3267. (e) Skvortsov, G. G.; Yakovenko, M. V.; Fukin, G. K.; Baranov, E. V.; Kurskii, Yu. A.; Trifonov, A. A. *Russ. Chem. Bull.* **2007**, *56*, 456–460.

(21) Further attempt to synthesize **10** by reaction of a 1:1 mixture of Y[N(SiMe<sub>3</sub>)<sub>2</sub>]<sub>3</sub> and LiN(SiMe<sub>3</sub>)<sub>2</sub> with 2 equiv of pro-ligand {LON<sup>Cy</sup>}H<sub>2</sub> yielded intractable mixtures of unidentified products.

(22) In addition to the abovementioned amine elimination syntheses, reactions between Y[N(SiMe<sub>3</sub>)<sub>2</sub>]<sub>3</sub> and pro-ligand {LON<sup>Pr</sup>}H<sub>2</sub> with different stoichiometries (1:2 and 1:3) were investigated. All of them afforded compound **11** along with complex mixtures of unidentified products.

(23) For recent references on group 3 metal amidinate chemistry, see: (a) Bambirra, S.; Perazzolo, F.; Boot, S. J.; Sciarone, T. J. J.; Meetsma, A.; Hessen, B. *Organometallics* **2008**, *27*, 704–712 and references cited therein. (b) Harder, S. *Dalton Trans.* **2010**, *39*, 6677–6681 and references cited therein.

(24) For group 4 metal amidinate chemistry, see: Hagadorn, J. R.; McNevin, M. J. *Organometallics* **2003**, *22*, 609–611 and references cited therein.

(25) (a) Chapurina, Yu.; Hannedouche, J.; Collin, J.; Guillot, R.; Schulz, E.; Trifonov, A. *Chem. Commun.* **2010**, 6918–6920. (b) Aillaud, I.; Lyubov, D.; Collin, J.; Guillot, R.; Hannedouche, J.; Schulz, E.; Trifonov, A. *Organometallics* **2008**, *27*, 5929–5936.

(26) For comparison, the corresponding Y–C(methyl) bond lengths in yttrium complexes are [Li(TMEDA)][{(Me<sub>3</sub>Si)<sub>2</sub>NC(N<sup>i</sup>Pr)<sub>2</sub>}<sub>2</sub>Y(μ-Me)<sub>2</sub>], 2.505(4) and 2.508(4) Å;<sup>11d</sup> [(Me<sub>3</sub>Si)<sub>2</sub>NC(NCy)<sub>2</sub>]Y[(μ-Me)<sub>2</sub>Li(TMEDA)]<sub>2</sub>, 2.5307(19) and 2.5410(16) Å;<sup>11g</sup> [(R)-C<sub>20</sub>H<sub>12</sub>(NC<sub>3</sub>H<sub>9</sub>)<sub>2</sub>](μ-Me)<sub>2</sub>Li(L)[(μ-Me)Li(L)] (L = TMEDA, THF, Et<sub>2</sub>O), 2.555(4), 2.530(4), 2.537(5), 2.517(3), 2.520(3), and 2.541(3) Å.<sup>25b</sup>

(27) Von Zelewsky, A. *Stereochemistry of Coordination Compounds*; Wiley: Chichester, U. K., 1996; p 78.

(28) Similar catalytic tests using *rac*-BBL as a monomer, carried out under regular conditions, revealed that all complexes are inactive.

(29) (a) Ajellal, N.; Carpentier, J.-F.; Guillaume, C.; Guillaume, S. M.; Helou, M.; Poirier, V.; Sarazin, Y. *Dalton Trans.* **2010**, *39*, 8363–8376. (b) Amgoune, A.; Thomas, C. M.; Carpentier, J.-F. *Macromol. Rapid Commun.* **2007**, *28*, 693–697.

(30) Manzer, L. E. *Inorg. Chem.* **1978**, *17*, 1552–1558.

(31) Bradley, D. C.; Ghotra, J. S.; Hart, F. A. *J. Chem. Soc., Dalton Trans.* **1973**, 1021–1023.

(32) (a) Barakat, I.; Dubois, P.; Jerome, R.; Teyssié, P. *J. Polym. Sci., A: Polym. Chem.* **1993**, *31*, 505–514.

(33) The amidine hydrogen could not be unambiguously detected by <sup>1</sup>H NMR.

(34) (a) Sheldrick, G. M. *SHELXS-97: Program for the Determination of Crystal Structures*; University of Goettingen: Goettingen, Germany, 1997. (b) Sheldrick, G. M. *SHELXL-97: Program for the Refinement of Crystal Structures*; University of Goettingen: Goettingen, Germany, 1997. (c) Sheldrick, G. M. *Acta Crystallogr.* **2008**, *A64*, 112.